Title
Robust gene expression changes in the ganglia following subclinical reactivation in rhesus macaques infected with simian varicella virus

Journal
Journal of NeuroVirology, 23(4)

ISSN
1355-0284

Authors
Arnold, Nicole
Meyer, Christine
Engelmann, Flora
et al.

Publication Date
2017-08-01

DOI
10.1007/s13365-017-0522-3

J. Neurovirol.
DOI 10.1007/s13365-017-0522-3

Robust gene expression changes in the ganglia following subclinical reactivation in rhesus macaques infected with simian varicella virus

Nicole Arnold[1,2] · Christine Meyer[3] · Flora Engelmann[1] · Ilhem Messaoudi[1,2,3]

Received: 14 November 2016 / Revised: 3 February 2017 / Accepted: 17 February 2017

Abstract Varicella zoster virus (VZV) causes varicella during acute infection and establishes latency in the sensory ganglia. Reactivation of VZV results in herpes zoster, a debilitating and painful disease. It is believed that VZV reactivates due to a decline in cell-mediated immunity; however, the roles that CD4 versus CD8 T cells play in the prevention of herpes zoster remain poorly understood. To address this question, we used a well-characterized model of VZV infection where rhesus macaques are intrabronchially infected with the homologous simian varicella virus (SVV). Latently infected rhesus macaques were thymectomized and depleted of either CD4 or CD8 T cells to induce selective senescence of each T cell subset. After T cell depletion, the animals were transferred to a new housing room to induce stress. SVV reactivation (viremia in the absence of rash) was detected in three out of six CD8-depleted and two out of six CD4-depleted animals suggesting that both CD4 and CD8 T cells play a critical role in preventing SVV reactivation. Viral loads in multiple ganglia were higher in reactivated animals compared to non-reactivated animals. In addition, reactivation results in sustained transcriptional changes in the ganglia that enriched to gene ontology and diseases terms associated with neuronal function and inflammation indicative of potential damage as a result of viral reactivation. These studies support the critical role of cellular immunity in preventing varicella virus reactivation and indicate that reactivation results in long-lasting remodeling of the ganglia transcriptome.

Keywords Latency · Herpesvirus · Herpes zoster · Sensory ganglia · RNA-Seq

Electronic supplementary material The online version of this article (doi:10.1007/s13365-017-0522-3) contains supplementary material, which is available to authorized users.

✉ Ilhem Messaoudi
imessaou@uci.edu

[1] Graduate Program in Microbiology, University of California-Riverside, Riverside, CA, USA

[2] Department of Molecular Biology and Biochemistry, Ayala School of Biological Sciences, University of California-Irvine, 2400 Biological Sciences III, Irvine, CA 92697-3900, USA

[3] Division of Pathobiology and Immunology, Oregon National Primate Research Center, Beaverton, OR, USA

Introduction

Varicella zoster virus (VZV) is a human neurotropic alpha herpesvirus that causes varicella (chicken pox) during primary infection. VZV establishes latency in the sensory ganglia where it can reactivate to cause herpes zoster (HZ, shingles). The risk of getting HZ significantly increases with age, from an average of 3 cases per 1000 adults 40–50 years old to 10 cases of HZ per 1000 adults aged ≥80 years (Keating 2013). In addition, the incidence of HZ in individuals receiving immunosuppressive drugs such as those with autoimmune diseases, cancer and organ transplant recipients is higher (Arvin 2000; Rusthoven et al. 1988; Wilson et al. 1972; Yawn et al. 2011). VZV has also been shown to reactivate following stressful situations (Schmader et al. 1990), such as during and after spaceflight (Cohrs et al. 2008) and in medical students (Uchakin et al. 2011).

It is generally believed that VZV reactivation is due to the loss of VZV-specific cell-mediated immunity (Terada et al. 1994), since antibody titers remain relatively stable with increasing age (Levin et al. 2008; Oxman 2009; Weinberg et al. 2009). Similarly, VZV reactivation in hematopoietic stem cell transplants was associated with low CD4 T cell counts in the absence of significant changes in antibody titers (Vermont

Published online: 20 March 2017

et al. 2014). Finally, T cell responses, but not antibody titers, negatively correlate with HZ disease severity (Onozawa et al. 2006; Park et al. 2004). However, the role of CD4 versus CD8 T cell immunity in preventing VZV reactivation is not well understood. Previous studies showed that the frequency of VZV-specific CD4 T cells declines more dramatically with age compared to VZV-specific CD8 T cells, suggesting a greater role for CD4 T cells in reactivation, but this hypothesis has yet to be formally tested (Asanuma et al. 2000; Weinberg et al. 2009).

In this study, we investigated the role of CD4 and CD8 T cell immunity in preventing herpes zoster using a non-human primate model of VZV infection. In this model, rhesus macaques are inoculated intrabronchially with simian varicella virus (SVV), a homologue of VZV. We previously showed that this model recapitulates the essential features of VZV infection in humans including varicella and establishment of latency in sensory ganglia (Messaoudi et al. 2009). Moreover, as described for VZV, SVV reactivates under conditions of immune suppression (Mahalingam et al. 2010; Mahalingam et al. 2007b; Ouwendijk et al. 2013; Traina-Dorge et al. 2015). To investigate the role that T cell senescence plays in SVV reactivation, rhesus macaques latently infected with SVV were first thymectomized and then depleted of either CD4 or CD8 T cells. This method leads to a profound loss of circulating T cells, which coupled with the absence of naïve T cell output (due to the thymectomy) results in robust homeostatic proliferation of the few T cells that have escaped depletion. This extensive proliferative burst accelerates T cell senescence in the depleted T cell population (Cho et al. 2000; Goldrath et al. 2000; Murali-Krishna and Ahmed 2000; Neujahr et al. 2006; Sheu et al. 2014). Finally, the animals were moved to a new room to induce stress.

SVV reactivation was detected in 42% of depleted animals (two CD4-depleted and three CD8-depleted animals). Moreover, average viral loads in the sensory ganglia from the animals that experienced a reactivation event were significantly higher. Finally, large gene expression changes were detected in ganglia collected from animals that underwent reactivation. Collectively, these data support the hypothesis that both CD4 and CD8 T cells play a critical role in preventing SVV reactivation and that SVV reactivation remodels the ganglia transcriptome.

Results

T cell depletion after thymectomy results in permanent loss of naïve T cells

Analysis of SVV replication kinetics and host responses in the 16 animals used in this study were previously published (Haberthur et al. 2014). All animals generated robust T and B cell responses as evidenced by the detection of antigen-specific T cells and antibodies (Haberthur et al. 2014). At 148 days post-infection (DPI), all 16 animals we thymectomized, and 29 days post-thymectomy (DPT), 12 animals were depleted of either CD4 or CD8 T cells (n = 6/group) while the remaining 4 animals served as thymectomized non-depleted controls. At 364 DPT, all animals were moved to a different room to induce environmental stress (Fig. 1a).

Thymectomy alone (control animals) had minimal impact on the frequency of circulating white blood cells (WBC) including lymphocytes and neutrophils (Fig. 1b–d). Similarly, thymectomy alone did not impact the frequency of circulating CD4 T, CD8 T, and CD20 B cells (Fig. 2a). Furthermore, very few changes were noted in the frequency of naïve and memory CD4 T, CD8 T, and B cell subsets (Fig. 2d, g, j). In contrast, CD4 depletion resulted in a significant decrease in the number of circulating lymphocytes (Fig. 1c) due to the loss of CD4 T cells (Fig. 2b) and, more specifically, naïve CD4 T cells (Fig. 2e), which remained significantly decreased for the remainder of the study. This change was accompanied by an increase in the frequency of terminally differentiated CD4 EM T cells (Fig. 2e). Frequency of CD8 T cells initially increased at 153 DPT in CD4-depleted animals but then decreased as CD4 numbers partially recovered (Fig. 2b). Interestingly, we also saw a significant increase in CD8 EM T cells and a decrease in naïve and TEM CD8 T cells in the CD4-depleted animals (Fig. 2h). No changes in B cell subsets were noted in the CD4-depleted animals (Fig. 2k).

As described for CD4 T cells, CD8 depletion resulted in a profound and sustained loss of CD8 T cells while the frequency of CD4 T cells and CD20 B cells remained relatively stable (Fig. 2c). This loss was also primarily driven by a significant reduction in the number of naïve CD8 T cells (Fig. 2i), which was accompanied by a transient increase in TEM CD8 T cells followed by an increase in the EM frequency (Fig. 2i). Intriguingly, the frequency of CD4 EM T cells increased while that of naïve and CM CD4 T cells decreased following CD8 depletion (Fig. 2f). The CD8-depleted animals had a significant increase in their switched memory B cell population after depletion (Fig. 2l).

T cells undergo robust homeostatic proliferation following depletion

The changes in frequency of naïve and memory T cells in the depleted animals prompted us to investigate the role of homeostatic proliferation. In the thymectomized non-depleted group, we observed a transient increase in proliferation in CD4 T cells and B cells, but not CD8 T cells 55–83 DPT (Fig. 3a–g). Following CD4 and CD8 T cell depletion, we observed robust proliferation in CD4 T, CD8 T, and B cells

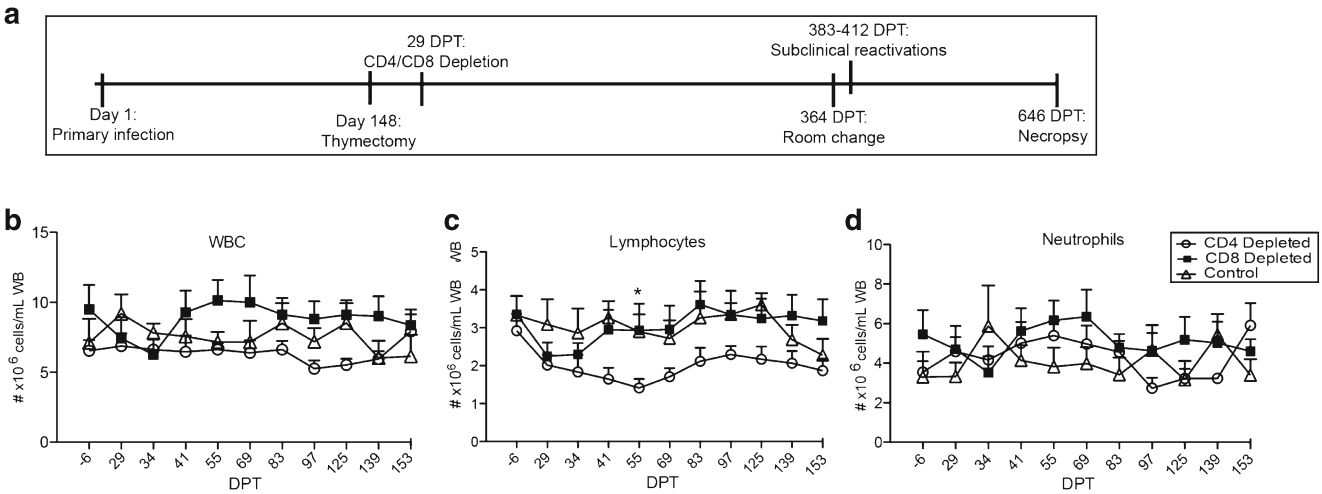

Fig. 1 Animal treatments and whole blood cell counts. **a** Experimental timeline. Absolute numbers of **b** white blood cells (WBC), **c** lymphocytes, and **d** neutrophils were measured in control ($n = 4$), CD4-depleted ($n = 6$), and CD8-depleted ($n = 6$) animals using a Hemavet. *Asterisk* $P < 0.05$ for CD4-depleted animals compared to day −6 post-thymectomy

as early as 29 DPT (Fig. 3). In the CD4-depleted animals, the magnitude of CD4 T cell proliferation was much more robust than that of CD8 T cells and B cells (Fig. 3b–h). Interestingly, in the CD8-depleted animals, CD4 T cell proliferation occurred earlier than CD8 T cell proliferation and reached similar magnitude (Fig. 3c, f). Although proliferation of naïve T cells was observed in both CD4-depleted and CD8-depleted groups, the naïve T cell numbers remained significantly reduced due to their rapid conversion to memory phenotype cells in the absence of thymic output.

T cell depletion followed by environmental stress results in subclinical reactivations

SVV reactivation was monitored by measuring SVV viral loads in the whole blood using quantitative real-time PCR (qPCR) as well as visual inspection for zoster lesions. After almost a year with no signs of reactivation, all of the animals were moved to a different room in the facility to induce stress (Fig. 1a). No obvious rash was detected in the animals; however, SVV DNA was detected in whole blood (WB) from five animals (two CD4 depleted (one male and one female) and three CD8 depleted (two male and one female)) approximately 20–48 days after the move (383–412 DPT) (Fig. 4a). To characterize the immune response during SVV reactivation, we measured changes in SVV-specific IgG titers and frequency of antigen-specific T cells. We observed no significant increases in IgG titers or CD4 T cell responses in the animals that experienced SVV reactivation (Fig. 4b–e). Increased CD8 T cell responses were detected in some of the depleted animals 412–454 DPT regardless of whether they experienced renewed viremia (Fig. 4f).

SVV reactivation results in increased viral loads and long-lasting transcriptional changes in the ganglia

No additional reactivation events were detected during the next several months. We therefore elected to euthanize the animals at 646 DPT and investigate changes in SVV viral loads and transcriptional profiles in the sensory ganglia following SVV reactivation. Significantly higher viral loads were observed in the trigeminal (TG) and dorsal root ganglia thoracic (DRG-T) of animals that showed signs of SVV reactivation compared to the animals that did not (Fig. 5a). No viral loads were detected in lumbar/sacral dorsal root ganglia (data not shown).

In order to determine the host transcriptome changes that occur following reactivation, we performed RNA-Seq on the DRG-T collected from three animals that experienced a reactivation event (two CD4 depleted, one CD8 depleted) and four animals that showed no signs of reactivation (two controls, one CD4 depleted and one CD8 depleted) (Table 1). A principle component analysis (PCA) showed a clear distinction between the reactivated and the control groups (Fig. 5b). Overall, we observed 1202 differentially expressed genes (DEGs) defined as having a fold change (FC) ≥2, a false discovery rate (FDR) of ≤0.05, and a median RPKM value of ≥5 (199 upregulated, 1003 downregulated) (Fig. 5c). To understand the biological implication of these transcriptional changes, we carried out a functional enrichment using Metacore™, which requires the use of human homologues. Of the 1202 DEGs, 641 had human homologues (120 upregulated and 521 downregulated) (Supplemental Dataset). Changes in expression of four DEGs were confirmed by RT-PCR (Fig. 6).

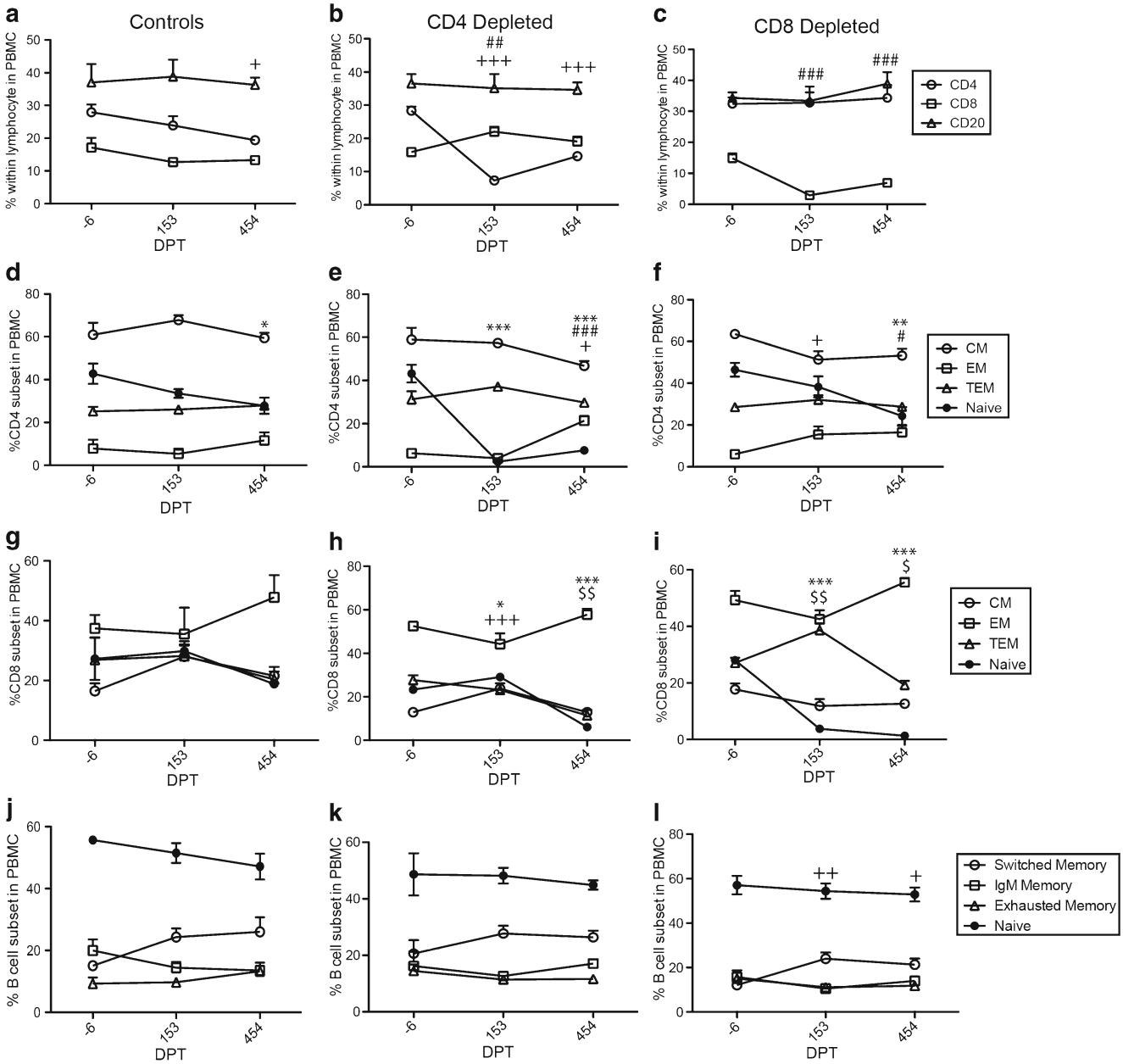

Fig. 2 Thymectomy followed by depletion results in the loss of naïve T cells. The frequencies of **a** CD4 T, **b** CD8 T, and **c** CD20 B cells (means ± SEM) were determined in the PBMC by flow cytometry (*three plus signs* $P < 0.001$ for CD4 T cells; *two number signs* $P < 0.01$; *three number signs* $P < 0.001$ for CD8 T cells). The frequencies of CM, EM, TEM, and naïve CD4 T cells in **d** control, **e** CD4-depleted, and **f** CD8-depleted animals and CD8 T cells in the **g** control, **h** CD4-depleted, and **i** CD8-depleted animals determined by flow cytometry (*one plus sign* $P < 0.05$, *two plus signs* $P < 0.01$, *three plus signs* $P < 0.001$ for CM; *one number sign* $P < 0.05$, *two number signs* $P < 0.01$, *three number signs* $P < 0.001$ for EM; *one dollar sign* $P < 0.05$, *two dollar signs* $P < 0.01$ for TEM; *one asterisk* $P < 0.05$, *two asterisks* $P < 0.01$, *three asterisks* $P < 0.001$ for naïve). The frequency (mean ± SEM) of class-switched memory, IgM memory, exhausted memory, and naïve B cells in the **j** control, **k** CD4-depleted, **l** CD8-depleted animals were determined by flow cytometry in PBMC (*one plus sign* $P < 0.05$, *two plus signs* $P < 0.01$, for switched memory) (controls, $n = 4$; CD4 depleted, $n = 6$; CD8 depleted, $n = 6$)

Genes upregulated in ganglia of animals that experienced SVV reactivation play a role in regulating cell cycle and gene expression

Only 120 characterized DEGs were found to be upregulated in ganglia of animals that experienced SVV reactivation. Several of the 30 most upregulated genes regulate cell cycle progression (Fig. 7a) such as *AMD1* (FC 4) which regulates Myc expression (Zhang et al. 2012), *POC1B* (FC 3) involved with centriole assembly (Keller et al. 2009), and the transcriptional regulator *TAF1D* (FC 4, confirmed by RT-PCR, Fig. 6a) (Wieczorek et al. 1998). Additional genes were involved with apoptosis such as *HIF1A* (FC 3) (Rapino et al. 2005) and *MAP4K5* (FC 3) (Iacobas et al. 2003), and protein degradation

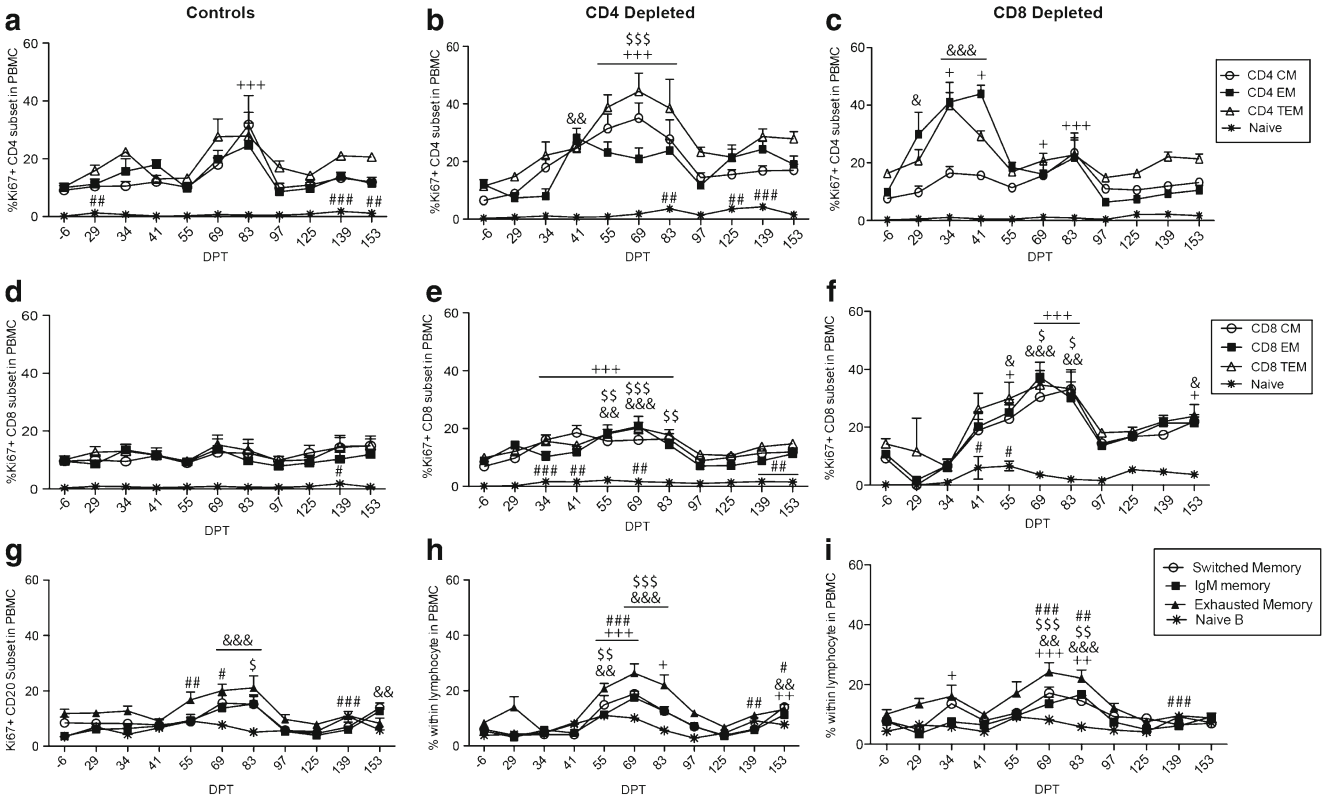

Fig. 3 Depletion results in robust homeostatic proliferation. Magnitude and kinetics of proliferation (means ± SEM) of CD4 T cell subsets were measured in **a** control, **b** CD4-depleted, and **c** CD8-depleted animals; CD8 T cell subsets in **d** control, **e** CD4-depleted, and **f** CD8-depleted animals; and B cell subsets in **g** control, **h** CD4-depleted, and **i** CD8-depleted animals were determined by measuring Ki67 expression within specific lymphocyte subsets by flow cytometry (*one plus sign* $P < 0.05$, *two plus signs* $P < 0.01$, *three plus signs* $P < 0.001$ for CM; *one ampersand* $P < 0.05$, *two ampersands* $P < 0.01$, *three ampersands* $P < 0.001$ for EM; *one dollar sign* $P < 0.05$, *two dollar signs* $P < 0.01$, *three dollar signs* $P < 0.001$ for TEM; *one number sign* $P < 0.05$, *two number signs* $P < 0.01$, *three number signs* $P < 0.001$ for naïve T cells; *one plus sign* $P < 0.05$, *two plus signs* $P < 0.01$, *three plus signs* $P < 0.001$ for switched memory; *two ampersands* $P < 0.01$, *three ampersands* $P < 0.001$ for IgM memory; *one dollar sign* $P < 0.05$, *two dollar signs* $P < 0.01$, *three dollar signs* $P < 0.001$ for exhausted memory; *one number sign* $P < 0.05$, *two number signs* $P < 0.01$, *three number signs* $P < 0.001$ for naïve B cells)

such as *UFD1L* (FC 3) (Johnson et al. 1995) and *CLPX* (FC 3) (Flynn et al. 2003). Other highly upregulated genes play a role in neuronal development such as *SNAPC3* (FC 3) (Wang et al. 2004), *OLIG3* (FC 3) (Liu et al. 2008), and *ACVR2A* (FC 3) (O'Keeffe et al. 2016) (Fig.7a). Two antiviral genes were also amongst the 30 most upregulated DEGs: *TRIM23* (FC 3), which enhances antiviral innate responses through the RIG-I/MDA5-mediated pathway (Arimoto et al. 2010), and *UFL1* (FC 4), which inhibits NF-kappaB signaling pathway (Kwon et al. 2010).

Functional enrichment showed that most of the upregulated DEGs mapped to "cellular metabolic process" (Table 2), some of which also enriched to GO term "response to glucose." Examples of genes that mapped to these two GO processes include those involved with double-stranded DNA damage repair (*BAZ1A*, FC 3) (Lan et al. 2010), transcriptional regulation (*MIER1*, FC 3) (Blackmore et al. 2008), mRNA degradation (*CNOT7*, FC 2) (Aslam et al. 2009), and regulation of circadian calcium rhythms in neurons (*ARNT*, FC 2) (Ikeda and Ikeda 2014). An additional 17 genes that mapped to "multicellular organismal reproductive process" played a role in microtubule stabilization (Emanuele and Stukenberg 2007) (*CEP57*, FC3, confirmed by RT-PCR, Fig. 6b), anion transport (*SLC26A8*, FC 3 (Lohi et al. 2002)), and neuron development (*RARB* FC 2 (Maden 2007)) (Fig. 7b).

Genes downregulated in ganglia of animals that experienced SVV reactivation may contribute to neuronal damage

Several of the downregulated genes play a role in neuronal development. The most downregulated gene in our data set was *GPR137* (FC 400, confirmed by RT-PCR, Fig. 6c), a G protein-coupled receptor essential for controlling pain transmission in the trigeminal ganglia (Manteniotis et al. 2013) (Fig. 8a). Several of the downregulated DEGs were involved with axon regeneration such as *NDEL1* (FC 123) (Toth et al. 2008), *AMIGO3* (FC 200) (Kuja-Panula et al. 2003), *THY-1* (FC 110) (confirmed by RT-PCR, Fig. 6d) (Rege and Hagood 2006), and *INA* (FC 89) (Baum and Garriga 1997). Additional

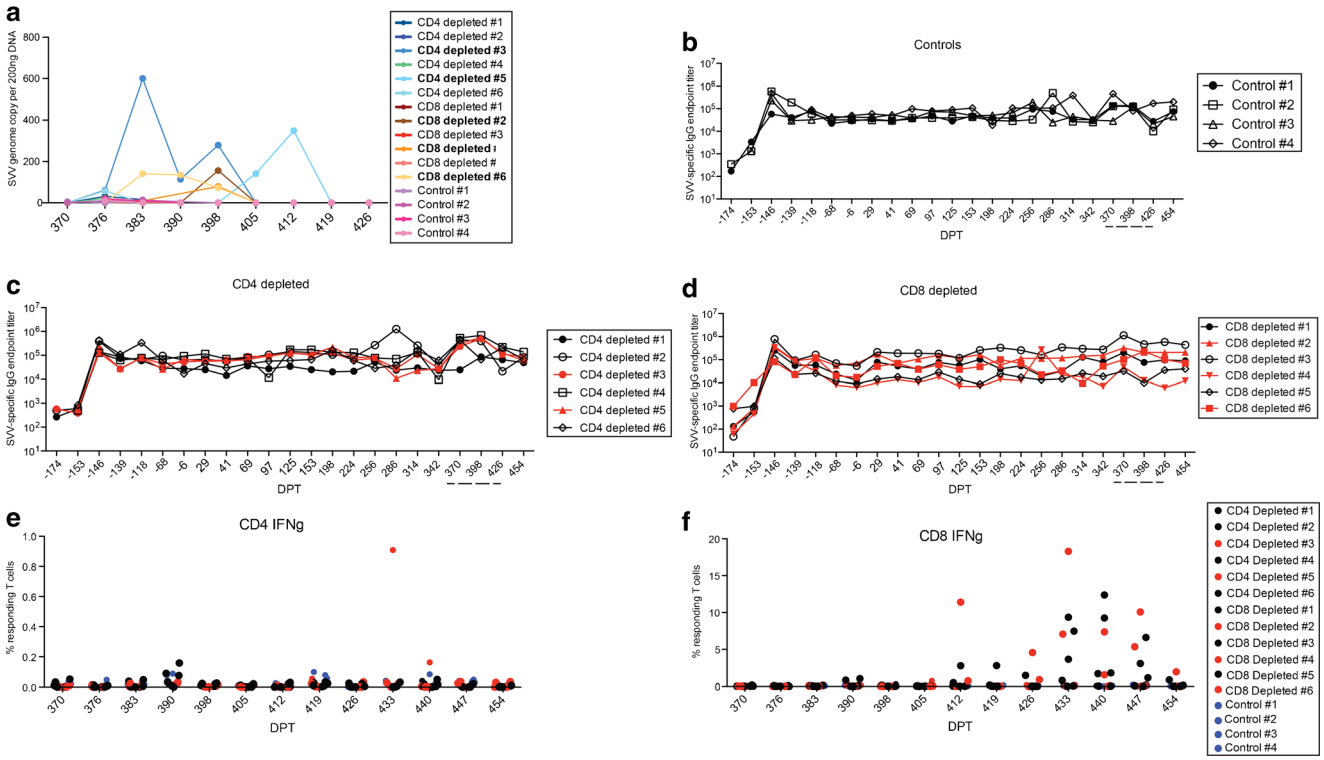

Fig. 4 SVV reactivation is detected in depleted animals in the absence of robust changes in immunity. **a** SVV DNA viral loads were assessed in PBMC (200 ng/sample). SVV-specific IgG titers were determined in **b** control, **c** CD4-depleted, and **d** CD8-depleted animals. Frequencies of PBMC SVV-specific **e** CD4 and **f** CD8 T cells producing IFNγ in animals that experienced SVV reactivation (*red*), depleted animals that did not experience a reactivation (*black*), and controls (*blue*). The *dashed line* represents the reactivation period

downregulated genes were involved in neuron differentiation and stabilization such as *FERD3L* (FC 104) (Ono et al. 2010), *BASP1* (FC 200) (Goodfellow et al. 2011), and *HSPA12B* (FC 119) (Ono et al. 2010). Finally, other highly downregulated genes played a role in cell proliferation (*MZF1*, FC 124) (Gaboli et al. 2001), DNA damage repair (*XRCC3*, FC 121) (Kurumizaka et al. 2001), and protein transport (*SSR4*, FC 183) (Nagasawa et al. 2007) (Fig. 8a).

Functional enrichment showed that the most statistically significant GO process to which downregulated DEGs mapped is "axo-dendritic-transport" which includes genes encoding neurofilaments *NEFL* (FC 7) and *NEFM* (FC 4), and the neurodevelopment protein *NDEL1* (FC 123) (Table 2). Several of the 215 downregulated genes that mapped to "cellular component organization" (Table 2) regulate neuronal gene expression including several histone genes (*HIST1H2AC* (FC 28), *HIST2H2AA4* (FC 70), *HIST2H3D* (FC 47), and *HIST3H2BB* (FC22) (Maze et al. 2015), as well as transcription factors such as *ATF5* (FC 158) (Angelastro et al. 2005) and *BAIAP2* (FC 155) (Oda et al. 1999). In addition, several highly downregulated genes mapped to "metabolic process" (Table 2) such as *PGAM2* (FC 149, glycolysis) (Kondoh et al. 2005), *CBR3* (FC 130, prostaglandin metabolism) (Miura et al. 2008), and *HEXIM2* (FC 54, transcription regulation) (Yik et al. 2005). Of the 177 genes that mapped to the GO process "response to stress," 43 directly interact with each other (Fig. 8b) including several that interact with the transcription factor *APP* (FC 7), which regulates neurite outgrowth (Bekris et al. 2011), and histone deacetylase class II (*HDAC*, FC 5).

Additional bioinformatics analysis of the downregulated DEGs revealed enrichment to process networks associated with the cell cycle (Table 2) including DNA repair such as *RAD9* (FC 44) (Lieberman et al. 1996); microtubule assembly, e.g., *TUBA1B* (FC 7) (Kumar et al. 2010); and cell cycle progression, e.g., *ANAPC13* (FC 9) (Yamaguchi et al. 2015). Several downregulated genes also enriched to the process network "immune response-antigen presentation" (Table 2) such as *ICAM* (FC 37), *NFKBIB* (FC 12), and several heat shock proteins (*HSPA1L* (FC 95), *HSPA8* (FC 8), *HSPCA* (FC 5), and *HSP90* (FC 2)) (Fig. 8c). Finally, analysis of the downregulated genes using a diseases biomarker database revealed enrichment to several diseases related to the neuronal damage and mental health diseases (Table 2). The DEGs that enriched to "basal ganglia diseases" played a role in axon regeneration such as *NGF* (FC10) (Lindsay 1988) and *SNCG* (FC 59) (Buckingham et al. 2008); neuron differentiation, e.g., *SUZ12* (FC6) (Mazzoni et al. 2013); and CNS inflammation such as *CCR7* (FC 8) (Buonamici et al. 2009) (Fig. 8d).

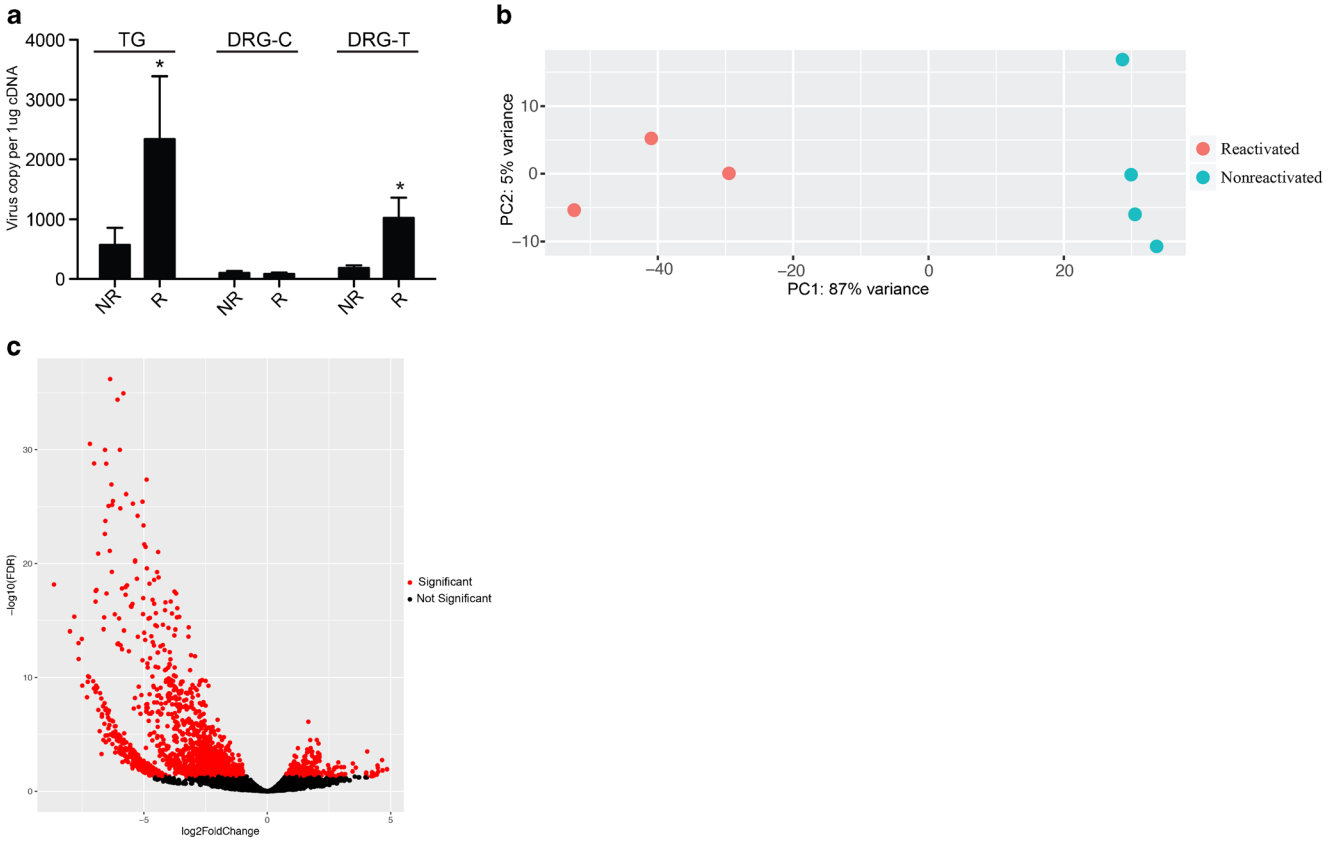

Fig. 5 SVV reactivation results in substantial host transcriptional changes in the ganglia. **a** SVV DNA viral loads were assessed in sensory ganglia (1 μg/sample) by quantitative real-time PCR using primers and probes specific for SVV ORF21 (*TG* trigeminal, *DRG-C* dorsal root ganglia cervical, *DRG-T* thoracic) (TG; $n = 6$ for animals that did not experience reactivation (*NR*), $n = 3$ for those that experienced reactivation (*R*); DRG-T; $n = 6$ for NR, $n = 5$ for R; DRG-C; $n = 6$ for NR and $n = 5$ for R). **b** PCA plot of the ganglia transcriptomes ($n = 3$ for R and $n = 4$ NR). **c** Volcano plot representing overall gene expression changes observed in animals that experienced renewed SVV viremia

SVV reactivation leads to greater changes in gene expression relative to latent SVV infection

We also compared changes in gene expression in ganglia collected from animals that experienced a reactivation event and those that did not relative to ganglia collected from naïve animals (Arnold et al. 2016). Overall, we detected 967 DEGs (403 upregulated, 325 downregulated) in ganglia from animals that did not have a reactivation and 1200 DEGs (641 upregulated, 559 downregulated) in the ganglia from animals that did. A comparison of these two data sets showed 728 genes were differentially expressed in ganglia obtained from either reactivated or non-reactivated animals relative to naïve ganglia, while 239 DEGs were only detected in ganglia of non-reactivated animals and 427 DEGs in ganglia from reactivated animals (Fig. 9a).

Functional enrichment was then performed on all three sets of DEGs to better understand the biological implications of these gene expression changes (Table 3). Genes that were differentially expressed in both sets of ganglia relative to naïve enriched to biological and disease processes related to metabolism, cell death, neurogenesis, and infections (Table 3). Most of the common genes mapped to "metabolic process" directly interacted with one another (Fig. 9a) and were regulated by the transcription factor NRF2, which regulates oxidative stress (Li et al. 2005) (Fig. 9b). In addition, all of the common genes that mapped to the disease process "infection" had the same directional change; however, DEGs detected in ganglia from animals that experienced a reactivation had a

Table 1 DRG-T viral loads of the samples used for RNA-Seq analysis

Sample	Reactivated	Viral load
CD4 depleted #3	Y	555
CD4 depleted #5	Y	189
CD8 depleted #6	Y	2091
Control #2	N	64
Control #3	N	236
CD4 depleted #6	N	152
CD8 depleted #5	N	21

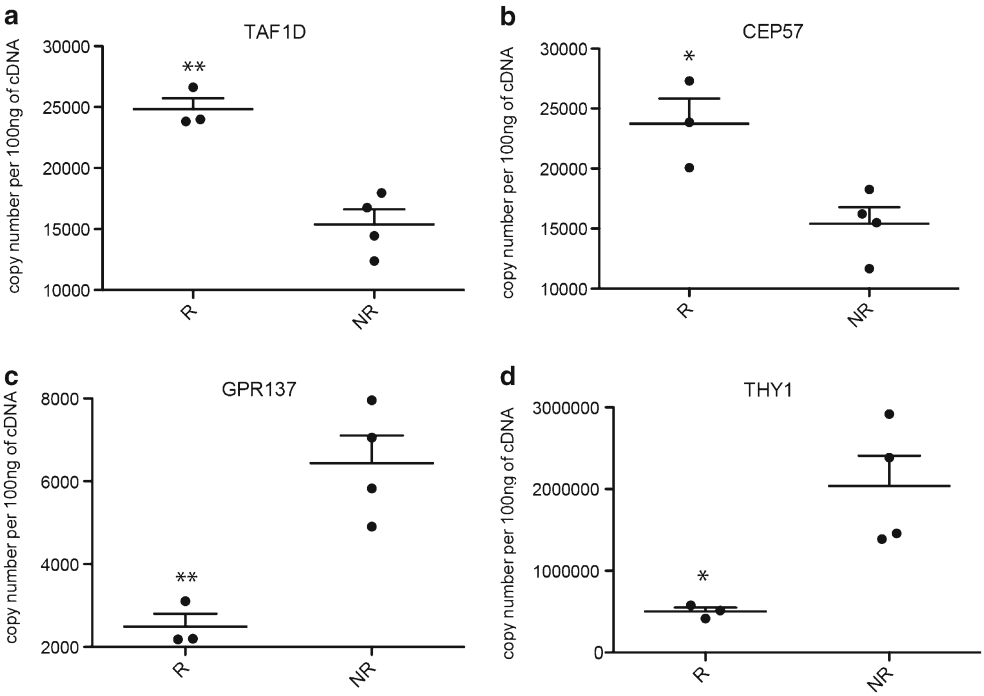

Fig. 6 Gene validation. Taqman assays were done on **a** TAF1D (upregulated), **b** GPR137 (downregulated), **c** THY1 (downregulated), and **d** CEP57 (upregulated). $n = 3$ for reactivated (*R*) and $n = 4$ for non-reactivation (*NR*). *One asterisk* $P < 0.05$, *two asterisks* $P < 0.01$ compared to NR

higher FC (Fig. 9c). The upregulated immune genes included antiviral genes such as *IFI16* and *DDX58*, T cell genes such as *IL-7* and *CD274*, and costimulatory molecules such as *CD80* and *CD46*. Downregulated immune genes included phagocytic markers *CD68* and *CD63*, as well as regulatory T cell transcription factor *FOXP3* (Fig. 9c). DEGs

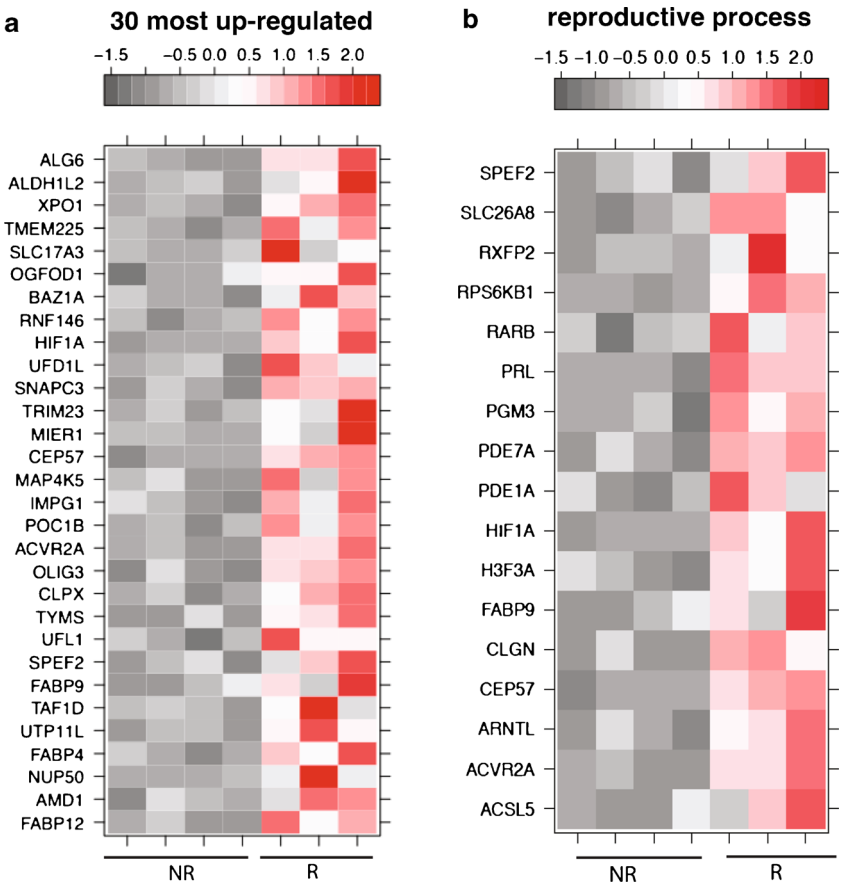

Fig. 7 Gene enrichment analysis of the upregulated genes in reactivated animals. Heat map analysis of the **a** 30 most upregulated and **b** upregulated genes mapping to "multicellular organismal reproductive process." *NR* non-reactivated, *R* reactivated

Table 2 Gene enrichment analysis of upregulated and downregulated genes

GO process	# genes	FDR
Upregulated		
cAMP catabolic process	2	4.951E−03
Multicellular organismal reproductive process	17	5.523E−03
Response to glucose	8	1.360E−02
Cellular metabolic process	72	1.819E−02
Downregulated		
Axo-dendritic transport	14	4.396E−07
Cellular component organization	244	4.396E−07
Metabolic process	378	7.202E−07
Chaperone-mediated autophagy	6	1.740E−06
Cytoskeleton-dependent intracellular transport	21	1.818E−06
Regulation of intracellular transport	51	2.803E−06
Response to stress	177	9.804E−06
Regulation of protein complex stability	6	1.114E−05
Process networks		
Protein folding_response to unfolded proteins	11	1.305E−03
Cytoskeleton_intermediate filaments	10	1.890E−02
Cell cycle_meiosis	10	8.081E−02
Cytoskeleton_regulation of cytoskeleton rearrangement	14	8.081E−02
Transcription_chromatin modification	11	8.081E−02
Immune response_antigen presentation	11	5.694E−01
Diseases		
Amyloid neuropathies	9	1.700E−10
Alzheimer disease, early onset	11	2.220E−06
Parkinsonian disorders	32	4.676E−06
Spinal cord diseases	28	1.109E−05
Movement disorders	49	1.109E−05
Polyneuropathies	18	1.646E−05
Gliosis	9	2.181E−05
Memory disorders	9	2.181E−05
Basal ganglia diseases	45	2.343E−05
Motor neuron disease	22	3.493E−05
Cerebral arterial diseases	10	5.023E−05

detected only in ganglia from non-reactivated animals also enriched to biological and disease processes related to metabolism, cell adhesion, central nervous diseases, and viral infections. Genes that enriched to "central nervous system diseases" and "viral infection" were primarily upregulated and played a role in neuron growth such as *NGF* (FC 7, regulates neuron growth) (Indo et al. 1996), *DSC1* (FC 95, neural circuit regulation (Zhang et al. 2013)), and *CYR61* (FC 6, dendrite growth (Malik et al. 2013)) (Fig. 9d). Interestingly, DEGs detected only in ganglia from reactivated animals enriched to biological and disease processes related to cell cycle and neurodegenerative diseases. Genes that mapped to "neurodegenerative diseases" played a role in neuro-transmission such as intermediate filaments (e.g., *NEFL*, FC 11 and *GFAP*, FC 293), neurotransmitters (e.g., *TAC1*, FC 14) and synaptic vesicle exocytosis (e.g., *CLPX2*, FC 80) (Fig. 9e).

Discussion

Age and immune status are the primary risk factors for getting herpes zoster. The goal of this study was to investigate the role of CD4 and CD8 T cell immunity in preventing herpes zoster. Using the rhesus macaque animal model of SVV infection, we were able to artificially age either the CD4 or CD8 T cell population in latently infected animals by performing a thymectomy followed by CD4 or CD8 T cell depletion. The profound loss of T cells coupled with the absence of naïve T cell output from the thymus results in robust

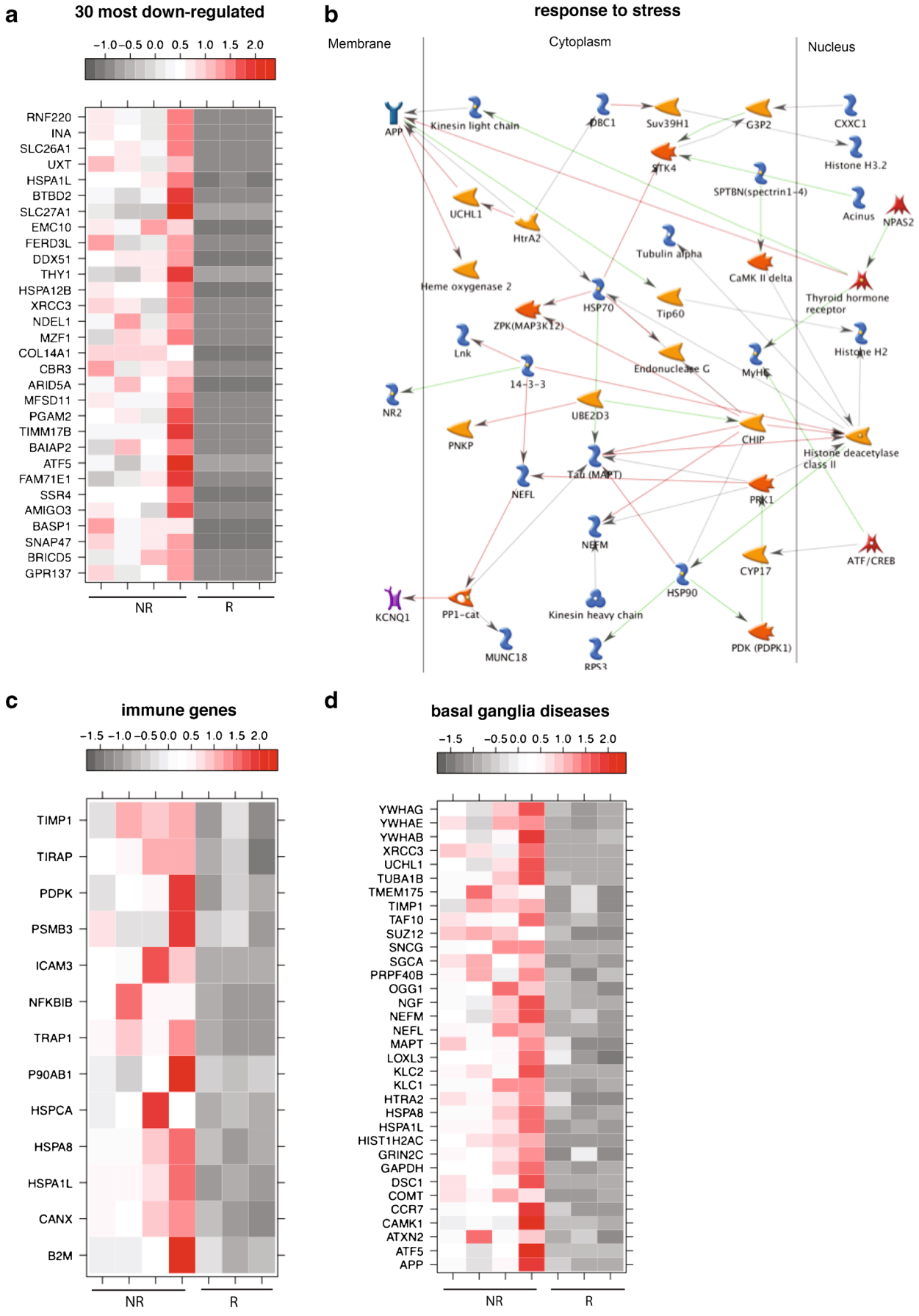
a
30 most down-regulated
−1.0 −0.5 0.0 0.5 1.0 1.5 2.0
RNF220
INA
SLC26A1
UXT
HSPA1L
BTBD2
SLC27A1
EMC10
FERD3L
DDX51
THY1
HSPA12B
XRCC3
NDEL1
MZF1
COL14A1
CBR3
ARID5A
MFSD11
PGAM2
TIMM17B
BAIAP2
ATF5
FAM71E1
SSR4
AMIGO3
BASP1
SNAP47
BRICD5
GPR137
NR
R
b
response to stress
Membrane
Cytoplasm
Nucleus
APP
Kinesin light chain
DBC1
Suv39H1
G3P2
CXXC1
Histone H3.2
STK4
SPTBN(spectrin1-4)
Acinus
NPAS2
UCHL1
HtrA2
Tubulin alpha
CaMK II delta
Heme oxygenase 2
HSP70
Tip60
Thyroid hormone receptor
ZPK(MAP3K12)
Lnk
Endonuclease G
MyHC
Histone H2
14-3-3
NR2
UBE2D3
PNKP
CHIP
Histone deacetylase class II
Tau (MAPT)
NEFL
PRK1
NEFM
CYP17
ATF/CREB
HSP90
KCNQ1
PP1-cat
Kinesin heavy chain
MUNC18
PDK (PDPK1)
c
immune genes
−1.5 −1.0 −0.5 0.0 0.5 1.0 1.5 2.0
TIMP1
TIRAP
PDPK
PSMB3
ICAM3
NFKBIB
TRAP1
P90AB1
HSPCA
HSPA8
HSPA1L
CANX
B2M
NR
R
d
basal ganglia diseases
−1.5 −0.5 0.0 0.5 1.0 1.5 2.0
YWHAG
YWHAE
YWHAB
XRCC3
UCHL1
TUBA1B
TMEM175
TIMP1
TAF10
SUZ12
SNCG
SGCA
PRPF40B
OGG1
NGF
NEFM
NEFL
MAPT
LOXL3
KLC2
KLC1
HTRA2
HSPA8
HSPA1L
HIST1H2AC
GRIN2C
GAPDH
DSC1
COMT
CCR7
CAMK1
ATXN2
ATF5
APP
NR
R

◀ **Fig. 8** Gene enrichment analysis of the downregulated genes in reactivated animals. **a** Heatmap analysis of the 30 most downregulated genes. **b** Network image showing the genes that directly interact in the downregulated genes found in the GO process "response to stress." **c** Heat map analysis of the downregulated immune genes. **d** Heat map analysis of the genes that mapped to GO process "basal ganglia diseases." *NR* non-reactivated, *R* reactivated

homeostatic proliferation in order to repopulate the T cell compartment, which in turn leads to accelerated T cell senescence (Cho et al. 2000; Goldrath et al. 2000; Murali-Krishna and Ahmed 2000; Neujahr et al. 2006; Sheu et al. 2014). Our data showed that T cell numbers of the depleted subset do not recover to baseline levels no matter how robust the homeostatic proliferation. Similar findings have been reported in mice depleted of their lymphocytes (Neujahr et al. 2006). Interestingly, we observed increased proliferation in the non-depleted T cell subset and B cells, suggesting all lymphocytes are able to sense and respond to the available space created by the depletion.

Thymectomy and accelerated aging of the T cell compartment alone were not sufficient to cause reactivation. This observation explains the relatively low rates of reactivation in older individuals ≥80 years of age where the reactivation rate is 10 per 1000 persons/year despite the uniform presence of immune senescence. Similarly, the rate of VZV reactivation in HIV+ subjects is 9.3 per 1000 persons/year (Blank et al. 2012; Pergam et al. 2011). We therefore induced stress by moving the animals to a different room in the facility. Although we were not able to measure cortisol levels, previous studies in non-human primates have shown that room changes increase cortisol levels in the feces and hair in rhesus macaques for up to 1 year (Davenport et al. 2008). Also, fecal cortisol increases have also been observed in chimpanzees moved to a new facility (Reimers et al. 2007). In addition, temporary moves of 2 days or less have also been shown to increase cortisol levels in rhesus, bonnet, and cynomolgus macaques as well (Novak et al. 2013).

SVV reactivation was observed in two (33%) CD4-depleted and three (50%) CD8-depleted animals as evidenced by the presence of SVV DNA in blood and increased viral loads in the ganglia. This is in line with the incidence rate of HZ in bone marrow transplant patients, which had been reported to reach 43% (Chen et al. 2014; Koc et al. 2000; Novak et al. 2013). However, our reactivation rates are lower than those observed in macaques that have undergone whole body irradiation coupled with immune-suppressive treatments (Mahalingam et al. 2010), in line with the reduced severity of immune suppression due to accelerated senescence of only one T cell compartment. In this study, we did not detect a zoster rash. VZV reactivation in the absence of rash is referred to as zoster sine herpete (Blumenthal et al. 2011) and has been reported in HIV-positive patients, bone marrow transplant recipients, patients with leukemia, astronauts, and cynomolgus macaques subjected to stress from travel and isolation (Birlea et al. 2011; Ljungman et al. 1986; Mahalingam et al. 2007a).

SVV reactivation was observed in both CD4- and CD8-depleted animals, which suggests a role for both CD4 and CD8 T cells in the prevention of reactivation. Viral loads in the blood seemed to be slightly higher in the CD4-depleted animals; however, since only two CD4-depleted animals experienced reactivations, we could not determine whether this increase was significant. These observations are in line with clinical studies that have indicated a critical role for CD4 T cells in prevention of VZV reactivation. Specifically, HZ is more prevalent in HIV+ patients (Onunu and Uhunmwangho 2004). Furthermore, rapid recovery of CD4 T cells, but not CD8 T cells, after stem cell transplants is associated with reduced rates of cytomegalovirus reactivation (Drylewicz et al. 2016). Previous studies from our lab have also shown a greater role for CD4 T cells in the resolution of acute SVV infection where CD4-depleted animals had higher viral loads and prolonged disease and are unable to establish latency in the ganglia (Haberthur et al. 2011; Meyer et al. 2013). On the other hand, CD8+ cells in the trigeminal ganglia play a critical role in the prevention of HSV-1 reactivation in mice (St Leger and Hendricks 2011), which indicates that immunological control of reactivation may differ between these two closely related viruses.

In contrast to what has been previously reported for VZV, no significant changes in antibody titers were detected during SVV reactivation. Similarly, no increase in SVV-specific CD4 T cell responses was detected in animals that experienced a reactivation event. On the other hand, CD8 T cell responses were increased in several depleted animals regardless of renewed SVV viremia, but in none of the non-depleted controls. This observation suggests that depleted animals were more susceptible to the stress induced by the room change, but only some of the animals experienced a reactivation. Our data differs from previous reports where increased T cell responses have been observed in transplant recipients following subclinical reactivations (Ljungman et al. 1986). Although we were unable to detect a robust immune response in the peripheral blood, SVV reactivations could have triggered a local immune response within the ganglia. Unfortunately, we were unable to address this question since the ganglia tissue was collected nearly 1 year after viremia was detected.

Viral loads were higher in the ganglia collected from animals that experienced a reactivation compared to those collected from animals that did not. The increased SVV viral loads could have been due to viral replication during reactivation as previously reported for VZV and SVV (Ouwendijk et al. 2013; Reichelt et al. 2008) and/or additional seeding of the ganglia after renewed SVV viremia. However, it is also possible that the viral loads in the ganglia of the reactivated animals were higher to begin with, which made them more susceptible to reactivation. In addition to increased viral loads,

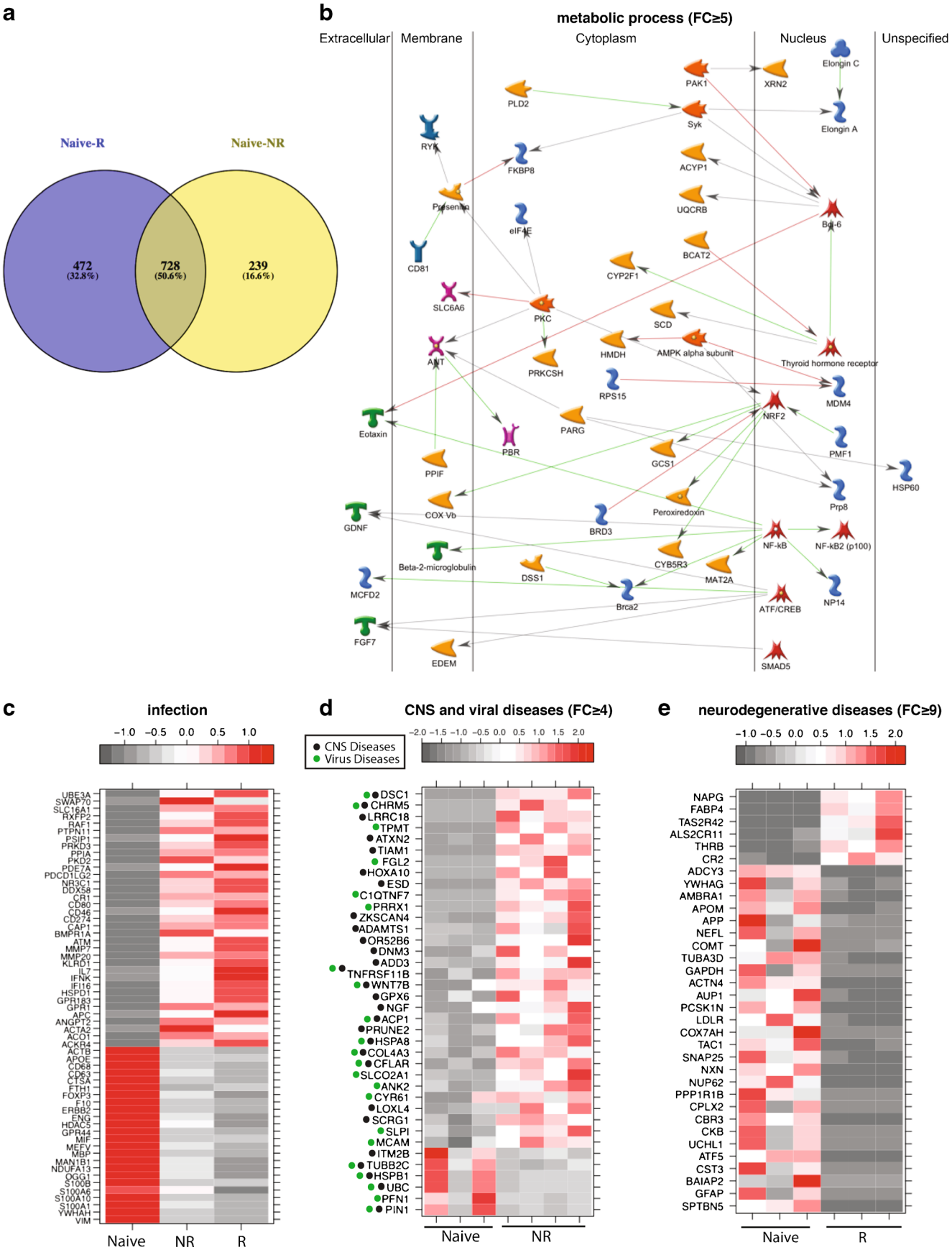
a
Naive-R
Naive-NR
472
(32.8%)
728
(50.6%)
239
(16.6%)
b
metabolic process (FC≥5)
Extracellular
Membrane
Cytoplasm
Nucleus
Unspecified
Elongin C
PAK1
XRN2
PLD2
Syk
Elongin A
RYK
FKBP8
ACYP1
Presenilin
UQCRB
Bcl-6
eIF4E
CD81
BCAT2
CYP2F1
SLC6A6
PKC
SCD
ANT
HMDH
AMPK alpha subunit
Thyroid hormone receptor
PRKCSH
RPS15
MDM4
Eotaxin
PARG
NRF2
PBR
PMF1
GCS1
HSP60
PPIF
Prp8
COX Vb
Peroxiredoxin
GDNF
BRD3
NF-kB
NF-kB2 (p100)
Beta-2-microglobulin
CYB5R3
DSS1
MAT2A
MCFD2
NP14
Brca2
ATF/CREB
FGF7
EDEM
SMAD5
c
infection
−1.0 −0.5 0.0 0.5 1.0
UBE3A
SWAP70
SLC16A1
RXFP2
RAF1
PTPN11
PSIP1
PRKD3
PPIA
PKD2
PDE7A
PDCD1LG2
NR3C1
DDX58
CR1
CD80
CD46
CD274
CAP1
BMPR1A
ATM
MMP7
MMP20
KLRD1
IL7
IFNK
IFI16
HSPD1
GPR183
GPR1
APC
ANGPT2
ACTA2
ACO1
ACKR4
ACTB
APOE
CD68
CD63
CTSA
FTH1
FOXP3
F10
ERBB2
ENG
HDAC5
GPR44
MIF
MEFV
MBP
MAN1B1
NDUFA13
OGG1
S100B
S100A6
S100A10
S100A1
YWHAH
VIM
Naive
NR
R
d
CNS and viral diseases (FC≥4)
CNS Diseases
Virus Diseases
−2.0 −1.5 −1.0 −0.5 0.0 0.5 1.0 1.5 2.0
DSC1
CHRM5
LRRC18
TPMT
ATXN2
TIAM1
FGL2
HOXA10
ESD
C1QTNF7
PRRX1
ZKSCAN4
ADAMTS1
OR52B6
DNM3
ADD3
TNFRSF11B
WNT7B
GPX6
NGF
ACP1
PRUNE2
HSPA8
COL4A3
CFLAR
SLCO2A1
ANK2
CYR61
LOXL4
SCRG1
SLPI
MCAM
ITM2B
TUBB2C
HSPB1
UBC
PFN1
PIN1
Naive
NR
e
neurodegenerative diseases (FC≥9)
−1.0 −0.5 0.0 0.5 1.0 1.5 2.0
NAPG
FABP4
TAS2R42
ALS2CR11
THRB
CR2
ADCY3
YWHAG
AMBRA1
APOM
APP
NEFL
COMT
TUBA3D
GAPDH
ACTN4
AUP1
PCSK1N
LDLR
COX7AH
TAC1
SNAP25
NXN
NUP62
PPP1R1B
CPLX2
CBR3
CKB
UCHL1
ATF5
CST3
BAIAP2
GFAP
SPTBN5
Naive
R

◀ **Fig. 9** Gene enrichment analysis on common and unique genes found in non-reactivated and reactivated animals compared to naïve animals. **a** Venn diagram of the DEGs from non-reactivated and reactivated animals. **b** Network image showing the common genes with a fold of at least five found in the GO process "metabolic process" that directly interact. **c** Heatmap of the common genes that mapped to "infection." **d** Heat map of the genes found only in the non-reactivated animals that mapped to disease process "central nervous system (CNS) diseases" and "virus diseases" with a fold change of at least four. **e** Heat map of the genes found only in the reactivated animals that mapped to disease process "neurodegenerative diseases" with a fold change of at least nine. *NR* non-reactivated, *R* reactivated

RNA-Seq analysis revealed distinct transcriptional profiles between the DRG-T of animals that experienced a reactivation event and those that did not despite the fact that our analysis was carried out 1 year after SVV viremia was detected. This suggests that SVV reactivations can cause long-lasting gene expression changes in the ganglia. Genes that were downregulated after reactivation play a critical role in neuron differentiation and axon regeneration as well as DNA repair indicative of significant damage to the ganglia, while genes that were upregulated after SVV reactivation play a role in cell proliferation and neuronal development, suggesting tissue repair. Although we were not able to examine the ganglia tissue at the time of reactivation, our gene expression data are supportive of previous studies that reported severe necrosis and inflammation of the ganglia recovered from patients with HZ at the time of death (Gowrishankar et al. 2010; Lungu et al. 1995).

Recent studies from our lab have shown a downregulation of neuronal genes during acute infection (Arnold et al. 2016); therefore, we compared the DEGs detected after acute SVV infection (100 dpi) and those detected after SVV reactivation. Only 48 common DEGs were identified, most of which were downregulated after both acute infection and reactivation. Several of these DEGs play a role in synaptic plasticity (*THRA*, *KIRREL*, and *IGFS8*) (Martin et al. 2015; Ray and Treloar 2012; Vallortigara et al. 2009), neuronal growth (*MBP*, *STMN2*, *PRPH*, and *RHOG*) (Eriksson et al. 2008; Franke et al. 2012; Westerlund et al. 2011), and cell cycle such as *ARF1*, *HDLBP*, and *BOP1* (Molyneux et al. 2014; Strezoska et al. 2000; Yorimitsu et al. 2014). Although a limited number of DEGs were shared between these studies, both revealed a robust number of downregulated genes that were involved in neuronal function, which suggests that both viral entry and viral reactivation cause neuronal damage but may affect different neuronal functions.

We also compared the transcriptome of ganglia from animals that experienced a reactivation and those that did not to ganglia from naïve animals. This analysis showed larger transcriptional changes in ganglia from animals that experienced a reactivation, further supporting the hypothesis that reactivation leads to additional remodeling of the ganglia transcriptome compared to latent SVV infection. A significant number of common DEGs were detected in ganglia from animals that experienced or did not experience a reactivation event, indicating that SVV infection exerts the largest transcriptional impact. In addition, several common genes enriched to infectious diseases; however, the reactivated ganglia showed larger gene expression changes in line with renewed viral replication such as that seen during reactivation. Additionally, we detected additional DEGs that were unique to ganglia from animals that experienced a reactivation. Genes that were differentially expressed only in ganglia from animals that experienced a reactivation event enriched to neurodegenerative diseases in line with the known complications of neuralgia and ganglia necrosis often observed after VZV reactivation (Gabutti et al. 2016).

In summary, data described in this study provides additional evidence that supports a critical role of T cells in the prevention of varicella virus reactivation. This study is also the first to characterize the gene expression changes that occur after SVV reactivation. Remarkably, significant changes in expression of genes important for neuronal function were altered nearly a year after reactivation, suggesting sustained remodeling of the ganglia transcriptome. These results provide additional insight into the development of post-herpetic neuralgia caused by neuronal damage that can last for years (Schmader 1998).

Methods

Animals and sample collection

Sixteen colony-bred Rhesus macaques (*Macaca mulatta*, RM) 3–4 years of age and of Indian origin were used in these studies. All the animals were housed and handled in accordance with the Oregon National Primate Research Center Institutional Animal Care and Use Committee (protocol #0779). The 16 RM were intrabronchially inoculated with 4×10^5 PFU SVV as previously described (Haberthur et al. 2014). At 148 days post-infection, all the animals were thymectomized. At 29, 32, and 37 DPT, six animals (two male and four female) were depleted of CD4 T cells using the humanized monoclonal antibody OKT4-HulgG at a dose of 50 mg/kg. Another six animals (two male and four female) were depleted of CD8 T cells using a mouse-human chimeric monoclonal antibody cM-T807 at a dose of 5 mg/kg on days 29, 32, and 37 post-thymectomy. The remaining four animals (all males) served as controls. All the animals were moved to a different room 364 DPT and were then euthanized ~646 DPT. All procedures were done under ketamine anesthesia to minimize pain. Necropsy was carried out in accordance with the recommendation of the American

Table 3 Gene enrichment analysis of non-reactivated and reactivated ganglia compared to naïve ganglia

GO process	# genes	FDR
DEGs detected in naïve verus ganglia from reactivated and non-reactivated animals		
Metabolic process	432	1.221E−09
Positive regulation of biological process	255	5.265E−06
Regulation of cell death	111	2.139E−05
Regulation of cellular component organization	107	8.362E−05
Process networks		
Muscle contraction	19	2.758E−02
Development neurogenesis axon guidance	21	7.962E−02
Diseases		
Infection	61	3.331E−04
Bacterial infections and mycoses	67	8.560E−04
Connective tissue diseases	123	1.65E−03
RNA virus infections	53	1.684E−03
DEGs detected only in naïve verus ganglia from non-reactivated animals		
Cell-cell adhesion	34	1.671E−03
Wnt signaling pathway, planar cell polarity pathway	9	6.722E−03
Regulation of type I interferon production	9	8.779E−03
Metabolic process	159	1.21E−02
Viral process	29	1.169E−02
Process networks		
Cytoskeleton_regulation of cytoskeleton rearrangement	12	1.80E−03
Cell adhesion_cell junctions	10	6.359E−03
Protein folding nucleus		
Cell cycle_meiosis	6	6.913E−03
Diseases		
Central nervous system diseases	53	3.314E−04
Virus diseases	38	4.470E−04
DNA virus infections	24	1.011E−03
Herpesviridae infections	15	2.827E−03
DEGs detected only in naïve verus ganglia from reactivated animals		
Metabolic process	323	7.163E−08
Cell cycle	79	2.076E−07
Organelle organization	146	3.141E−07
Regulation of synaptic plasticity	21	2.93E−05
Process networks		
Signal transduction_ESR1-nuclear pathway	13	1.579E−02
Protein folding_folding in normal condition	10	6.954E−02
Neurophysiological process_long-term potentiation	8	6.954E−02
Diseases		
Basal ganglia diseases	39	3.423E−08
Gliosis	5	3.603E−08
Cerebral arterial diseases	5	1.193E−07
Neurodegenerative diseases	77	5.964E−04
Trigeminal neuralgia	5	3.881E−06

Veterinary Association guidelines for euthanasia. Sensory ganglia tissue (trigeminal, dorsal root ganglia (DRG)-cervical, DRG-thoracic, and DRG-lumbar sacral) was collected at necropsy. Tissues were then flash frozen or stored in trizol at −80°. Peripheral blood mononuclear cells (PBMC) were isolated over a density gradient cell separation medium (Corning, Manassas, VA) and resuspended in RPMI with 10% FBS and PSG.

DNA extraction and viral loads

DNA was extracted from whole blood using the Qiagen genomic DNA extraction kit (Qiagen, Valencia, CA). Ganglia tissue was digested in proteinase K solution (20 mg/ml) overnight, and DNA was extracted using the Qiagen genomic DNA extraction kit (Qiagen, Valencia, CA). Viral loads were determined as previously described by real-time PCR using primers and probes specific for ORF21 and measured on the ABI StepOne instrument (Applied Biosystems, Foster City, CA).

Identification of immune cell populations

PBMC cells were stained with antibodies against CD8β (Beckman Coulter), CD4 (eBioscience, San Diego, CA), CD28 (BioLegend), CD95 (BioLegend), and CCR7 (BD Pharmingen), which allowed the delineation of central memory (CM; $CD28^+$ $CD95^+$ $CCR7^+$), transitional effector memory (TEM; $CD28^+$ $CD95^+$ $CCR7^-$), and effector memory (EM; $CD28^-$ $CD95^+$ $CCR7^-$) CD4 and CD8 T cells. PBMC cells were also surface stained with antibodies against CD20, IgD (Southern Biotech, Birmingham, AL) and CD27 (Biolegend) to delineate IgM (IgD+ CD27+), class-switched memory (IgD− CD27+), exhausted memory (IgD− CD27−), and naïve (igD= CD27−) B cell subsets. Cells were fixed and permeabilized according to manufacturer recommendations (BioLegend) before the addition of a Ki67-specific antibody (BD Pharmingen). The samples were analyzed using the LSRII instrument (Becton, Dickinson and Company, San Jose, CA) and FlowJo software (TreeStar, Ashland, OR).

Intracellular cytokine staining

PBMC were stimulated ex vivo with SVV lysate (1 μg) in the presence of brefeldin A (Sigma, St. Louis, MO) for 14 h. Cells were then stained with antibodies against CD4 and CD8β. Cells were then fixed, permeabilized (BioLegend), and stained for IFN-γ (eBioscience) and TNF-α (eBioscience). Samples were then acquired on the LSRII instrument and data was analyzed using FlowJo software.

RNA-sequencing analysis

RNA was extracted from ganglia tissue homogenized in trizol using a bead beater and zirconia/silica beads followed by extraction using the Ambion Purelink RNA Mini Kit (Life Technologies, Carlsbad, CA). RNA library preparation was done using the NEXTflex® Rapid Directional RNA-Seq kit (BIOO Scientific, Austin, TX). DNA libraries were then multiplexed and sequenced on the Illumina HiSeq2500 (Illumina, San Diego, CA) platform. All data analysis steps were performed with the RNA-Seq workflow module of the *systemPiperR* package available on Bioconductor (Girke 2015; Huber et al. 2015). Next-generation sequencing (NGS) quality reports were generated with the *seeFastq* function defined by the same package. RNA-Seq reads were mapped with the splice junction aware short read alignment suite Bowtie2/Tophat2 (Kim et al. 2013; Langmead and Salzberg 2012) against the *Macaca mulatta* genome sequence downloaded from Ensembl (Cunningham et al. 2015). The default parameters of Tophat2 optimized for mammalian genomes were used for the alignments. Raw expression values in the form of gene-level read counts were generated with the *summarizeOverlaps* function (Lawrence et al. 2013). Only reads overlapping the exonic regions of genes were counted, while reads mapping to ambiguous regions of exons from overlapping genes were discarded. Analysis of differentially expressed genes (DEGs) was performed with the GLM method from the *edgeR* package (Anders et al. 2013; Robinson et al. 2010) (SRP097695). For comparison to naïve ganglia, we leveraged RNA-Seq data from our recent publication (SRP072525 (Arnold et al. 2016)). In all analyses, differentially expressed genes (DEGs) were defined as those with a fold change ≥2, a false discovery rate (FDR) ≤0.05, and a median RPKM value ≥5. Enrichment analysis was performed using MetaCore software (GeneGo, Philadelphia, PA).

Gene expression change validation

RNA was reverse transcribed using random hexamers and SuperScript ® IV RT using the SuperScript ® IV First-Strand Synthesis System (Invitrogen, Lithuania) to generate cDNA. Taqman gene expression assays (Thermo Fisher, Waltham, MA) of selected genes and housekeeping gene (RPL32) were carried out using 100 ng of cDNA in duplicate on the ABI StepOne instrument (Applied Biosystems). mRNA expression levels were calculated relative to our housekeeping gene (RPL32) using $2^{-}\Delta Ct$ calculations.

Statistical analysis

Graphing was performed with GraphPad Prism software (GraphPad Software Inc., La Jolla, CA). One-way repeated-measures analysis of variance (ANOVA) with Dunnett's multiple comparison post-test was used to explore differences relative to and pre-thymectomy (−6 DPT) values. Unpaired *t* test was used to determine significance of ganglia viral loads and gene validation.

Acknowledgements We would like to thank Vanessa Rico for her help with blood processing and some of the flow cytometry assays. This work was funded by the National Institute of Health (NIH) (R01AG037042-06).

Compliance with ethical standards

Conflict of interest The authors declare that they have no conflict of interest.

References

Anders S, McCarthy DJ, Chen Y, Okoniewski M, Smyth GK, Huber W, Robinson MD (2013) Count-based differential expression analysis of RNA sequencing data using R and Bioconductor. Nat Protoc 8: 1765–1786

Angelastro JM, Mason JL, Ignatova TN, Kukekov VG, Stengren GB, Goldman JE, Greene LA (2005) Downregulation of activating transcription factor 5 is required for differentiation of neural progenitor cells into astrocytes. J Neurosci 25:3889–3899

Arimoto K, Funami K, Saeki Y, Tanaka K, Okawa K, Takeuchi O, Akira S, Murakami Y, Shimotohno K (2010) Polyubiquitin conjugation to NEMO by triparite motif protein 23 (TRIM23) is critical in antiviral defense. Proc Natl Acad Sci U S A 107:15856–15861

Arnold N, Girke T, Sureshchandra S, Messaoudi I (2016) Acute simian varicella virus infection causes robust and sustained changes in gene expression in the sensory ganglia. J Virol 90:10823–10843

Arvin AM (2000) Varicella-zoster virus: pathogenesis, immunity, and clinical management in hematopoietic cell transplant recipients. Biol Blood Marrow Transplant 6:219–230

Asanuma H, Sharp M, Maecker HT, Maino VC, Arvin AM (2000) Frequencies of memory T cells specific for varicella-zoster virus, herpes simplex virus, and cytomegalovirus by intracellular detection of cytokine expression. J Infect Dis 181:859–866

Aslam A, Mittal S, Koch F, Andrau JC, Winkler GS (2009) The Ccr4-NOT deadenylase subunits CNOT7 and CNOT8 have overlapping roles and modulate cell proliferation. Mol Biol Cell 20:3840–3850

Baum PD, Garriga G (1997) Neuronal migrations and axon fasciculation are disrupted in ina-1 integrin mutants. Neuron 19:51–62

Bekris LM, Galloway NM, Millard S, Lockhart D, Li G, Galasko DR, Farlow MR, Clark CM, Quinn JF, Kaye JA, Schellenberg GD, Leverenz JB, Seubert P, Tsuang DW, Peskind ER, Yu CE (2011) Amyloid precursor protein (APP) processing genes and cerebrospinal fluid APP cleavage product levels in Alzheimer's disease. Neurobiol Aging 32(556):e13–e23

Birlea M, Arendt G, Orhan E, Schmid DS, Bellini WJ, Schmidt C, Gilden D, Cohrs RJ (2011) Subclinical reactivation of varicella zoster virus in all stages of HIV infection. J Neurol Sci 304:22–24

Blackmore TM, Mercer CF, Paterno GD, Gillespie LL (2008) The transcriptional cofactor MIER1-beta negatively regulates histone acetyltransferase activity of the CREB-binding protein. BMC Res Notes 1:68

Blank LJ, Polydefkis MJ, Moore RD, Gebo KA (2012) Herpes zoster among persons living with HIV in the current antiretroviral therapy era. J Acquir Immune Defic Syndr 61:203–207

Blumenthal DT, Shacham-Shmueli E, Bokstein F, Schmid DS, Cohrs RJ, Nagel MA, Mahalingam R, Gilden D (2011) Zoster sine herpete: virologic verification by detection of anti-VZV IgG antibody in CSF. Neurology 76:484–485

Buckingham BP, Inman DM, Lambert W, Oglesby E, Calkins DJ, Steele MR, Vetter ML, Marsh-Armstrong N, Horner PJ (2008) Progressive ganglion cell degeneration precedes neuronal loss in a mouse model of glaucoma. J Neurosci 28:2735–2744

Buonamici S, Trimarchi T, Ruocco MG, Reavie L, Cathelin S, Mar BG, Klinakis A, Lukyanov Y, Tseng JC, Sen F, Gehrie E, Li M, Newcomb E, Zavadil J, Meruelo D, Lipp M, Ibrahim S, Efstratiadis A, Zagzag D, Bromberg JS, Dustin ML, Aifantis I (2009) CCR7 signalling as an essential regulator of CNS infiltration in T-cell leukaemia. Nature 459:1000–1004

Chen SY, Suaya JA, Li Q, Galindo CM, Misurski D, Burstin S, Levin MJ (2014) Incidence of herpes zoster in patients with altered immune function. Infection 42:325–334

Cho BK, Rao VP, Ge Q, Eisen HN, Chen J (2000) Homeostasis-stimulated proliferation drives naive T cells to differentiate directly into memory T cells. J Exp Med 192:549–556

Cohrs RJ, Mehta SK, Schmid DS, Gilden DH, Pierson DL (2008) Asymptomatic reactivation and shed of infectious varicella zoster virus in astronauts. J Med Virol 80:1116–1122

Cunningham F, Amode MR, Barrell D, Beal K, Billis K, Brent S, Carvalho-Silva D, Clapham P, Coates G, Fitzgerald S, Gil L, Giron CG, Gordon L, Hourlier T, Hunt SE, Janacek SH, Johnson N, Juettemann T, Kahari AK, Keenan S, Martin FJ, Maurel T, McLaren W, Murphy DN, Nag R, Overduin B, Parker A, Patricio M, Perry E, Pignatelli M, Riat HS, Sheppard D, Taylor K, Thormann A, Vullo A, Wilder SP, Zadissa A, Aken BL, Birney E, Harrow J, Kinsella R, Muffato M, Ruffier M, Searle SM, Spudich G, Trevanion SJ, Yates A, Zerbino DR, Flicek P (2015) Ensembl 2015. Nucleic Acids Res 43:D662–D669

Davenport MD, Lutz CK, Tiefenbacher S, Novak MA, Meyer JS (2008) A rhesus monkey model of self-injury: effects of relocation stress on behavior and neuroendocrine function. Biol Psychiatry 63:990–996

Drylewicz J, Schellens IM, Gaiser R, Nanlohy NM, Quakkelaar ED, Otten H, van Dorp S, Jacobi R, Ran L, Spijkers S, Koning D, Schuurman R, Meijer E, Pietersma FL, Kuball J, van Baarle D (2016) Rapid reconstitution of CD4 T cells and NK cells protects against CMV-reactivation after allogeneic stem cell transplantation. J Transl Med 14:230

Emanuele MJ, Stukenberg PT (2007) Xenopus Cep57 is a novel kinetochore component involved in microtubule attachment. Cell 130: 893–905

Eriksson KS, Zhang S, Lin L, Lariviere RC, Julien JP, Mignot E (2008) The type III neurofilament peripherin is expressed in the tuberomammillary neurons of the mouse. BMC Neurosci 9:26

Flynn JM, Neher SB, Kim YI, Sauer RT, Baker TA (2003) Proteomic discovery of cellular substrates of the ClpXP protease reveals five classes of ClpX-recognition signals. Mol Cell 11:671–683

Franke K, Otto W, Johannes S, Baumgart J, Nitsch R, Schumacher S (2012) miR-124-regulated RhoG reduces neuronal process complexity via ELMO/Dock180/Rac1 and Cdc42 signalling. EMBO J 31:2908–2921

Gaboli M, Kotsi PA, Gurrieri C, Cattoretti G, Ronchetti S, Cordon-Cardo C, Broxmeyer HE, Hromas R, Pandolfi PP (2001) Mzf1 controls cell proliferation and tumorigenesis. Genes Dev 15:1625–1630

Gabutti G, Bonanni P, Conversano M, Fanelli G, Franco E, Greco D, Icardi G, Lazzari M, Rossi A, Scotti S, Volpi A (2016). Prevention of herpes zoster and its complications: from clinical evidence to real life experience. Hum Vaccin Immunother: 0

Girke T (2015). systemPipeR:NGS workflow and report generation environment.

Goldrath AW, Bogatzki LY, Bevan MJ (2000) Naive T cells transiently acquire a memory-like phenotype during homeostasis-driven proliferation. J Exp Med 192:557–564

Goodfellow SJ, Rebello MR, Toska E, Zeef LA, Rudd SG, Medler KF, Roberts SG (2011) WT1 and its transcriptional cofactor BASP1 redirect the differentiation pathway of an established blood cell line. Biochem J 435:113–125

Gowrishankar K, Steain M, Cunningham AL, Rodriguez M, Blumbergs P, Slobedman B, Abendroth A (2010) Characterization of the host immune response in human ganglia after herpes zoster. J Virol 84: 8861–8870

Haberthur K, Engelmann F, Park B, Barron A, Legasse A, Dewane J, Fischer M, Kerns A, Brown M, Messaoudi I (2011) CD4 T cell immunity is critical for the control of simian varicella virus infection in a nonhuman primate model of VZV infection. PLoS Pathog 7: e1002367

Haberthur K, Meyer C, Arnold N, Engelmann F, Jeske DR, Messaoudi I (2014) Intrabronchial infection of rhesus macaques with simian varicella virus results in a robust immune response in the lungs. J Virol 88:12777–12792

Huber W, Carey VJ, Gentleman R, Anders S, Carlson M, Carvalho BS, Bravo HC, Davis S, Gatto L, Girke T, Gottardo R, Hahne F, Hansen

KD, Irizarry RA, Lawrence M, Love MI, MacDonald J, Obenchain V, Oles AK, Pages H, Reyes A, Shannon P, Smyth GK, Tenenbaum D, Waldron L, Morgan M (2015) Orchestrating high-throughput genomic analysis with Bioconductor. Nat Methods 12:115–121

Iacobas DA, Urban-Maldonado M, Iacobas S, Scemes E, Spray DC (2003) Array analysis of gene expression in connexin-43 null astrocytes. Physiol Genomics 15:177–190

Ikeda M, Ikeda M (2014) Bmal1 is an essential regulator for circadian cytosolic Ca(2)(+) rhythms in suprachiasmatic nucleus neurons. J Neurosci 34:12029–12038

Indo Y, Tsuruta M, Hayashida Y, Karim MA, Ohta K, Kawano T, Mitsubuchi H, Tonoki H, Awaya Y, Matsuda I (1996) Mutations in the TRKA/NGF receptor gene in patients with congenital insensitivity to pain with anhidrosis. Nat Genet 13:485–488

Johnson ES, Ma PC, Ota IM, Varshavsky A (1995) A proteolytic pathway that recognizes ubiquitin as a degradation signal. J Biol Chem 270: 17442–17456

Keating GM (2013) Shingles (herpes zoster) vaccine (zostavax(®)): a review of its use in the prevention of herpes zoster and postherpetic neuralgia in adults aged ≥50 years. Drugs 73:1227–1244

Keller LC, Geimer S, Romijn E, Yates J 3rd, Zamora I, Marshall WF (2009) Molecular architecture of the centriole proteome: the conserved WD40 domain protein POC1 is required for centriole duplication and length control. Mol Biol Cell 20:1150–1166

Kim D, Pertea G, Trapnell C, Pimentel H, Kelley R, Salzberg SL (2013) TopHat2: accurate alignment of transcriptomes in the presence of insertions, deletions and gene fusions. Genome Biol 14:R36

Koc Y, Miller KB, Schenkein DP, Griffith J, Akhtar M, DesJardin J, Snydman DR (2000) Varicella zoster virus infections following allogeneic bone marrow transplantation: frequency, risk factors, and clinical outcome. Biol Blood Marrow Transplant 6:44–49

Kondoh H, Lleonart ME, Gil J, Wang J, Degan P, Peters G, Martinez D, Carnero A, Beach D (2005) Glycolytic enzymes can modulate cellular life span. Cancer Res 65:177–185

Kuja-Panula J, Kiiltomaki M, Yamashiro T, Rouhiainen A, Rauvala H (2003) AMIGO, a transmembrane protein implicated in axon tract development, defines a novel protein family with leucine-rich repeats. J Cell Biol 160:963–973

Kumar RA, Pilz DT, Babatz TD, Cushion TD, Harvey K, Topf M, Yates L, Robb S, Uyanik G, Mancini GM, Rees MI, Harvey RJ, Dobyns WB (2010) TUBA1A mutations cause wide spectrum lissencephaly (smooth brain) and suggest that multiple neuronal migration pathways converge on alpha tubulins. Hum Mol Genet 19:2817–2827

Kurumizaka H, Ikawa S, Nakada M, Eda K, Kagawa W, Takata M, Takeda S, Yokoyama S, Shibata T (2001) Homologous-pairing activity of the human DNA-repair proteins Xrcc3.Rad51C. Proc Natl Acad Sci U S A 98:5538–5543

Kwon J, Cho HJ, Han SH, No JG, Kwon JY, Kim H (2010) A novel LZAP-binding protein, NLBP, inhibits cell invasion. J Biol Chem 285:12232–12240

Lan L, Ui A, Nakajima S, Hatakeyama K, Hoshi M, Watanabe R, Janicki SM, Ogiwara H, Kohno T, Kanno S, Yasui A (2010) The ACF1 complex is required for DNA double-strand break repair in human cells. Mol Cell 40:976–987

Langmead B, Salzberg SL (2012) Fast gapped-read alignment with Bowtie 2. Nat Methods 9:357–359

Lawrence M, Huber W, Pages H, Aboyoun P, Carlson M, Gentleman R, Morgan MT, Carey VJ (2013) Software for computing and annotating genomic ranges. PLoS Comput Biol 9:e1003118

Levin MJ, Oxman MN, Zhang JH, Johnson GR, Stanley H, Hayward AR, Caulfield MJ, Irwin MR, Smith JG, Clair J, Chan IS, Williams H, Harbecke R, Marchese R, Straus SE, Gershon A, Weinberg A (2008) Varicella-zoster virus-specific immune responses in elderly recipients of a herpes zoster vaccine. J Infect Dis 197:825–835

Li J, Johnson D, Calkins M, Wright L, Svendsen C, Johnson J (2005) Stabilization of Nrf2 by tBHQ confers protection against oxidative stress-induced cell death in human neural stem cells. Toxicol Sci 83: 313–328

Lieberman HB, Hopkins KM, Nass M, Demetrick D, Davey S (1996) A human homolog of the Schizosaccharomyces pombe rad9+ checkpoint control gene. Proc Natl Acad Sci U S A 93:13890–13895

Lindsay RM (1988) Nerve growth factors (NGF, BDNF) enhance axonal regeneration but are not required for survival of adult sensory neurons. J Neurosci 8:2394–2405

Liu Z, Li H, Hu X, Yu L, Liu H, Han R, Colella R, Mower GD, Chen Y, Qiu M (2008) Control of precerebellar neuron development by Olig3 bHLH transcription factor. J Neurosci 28:10124–10133

Ljungman P, Lonnqvist B, Gahrton G, Ringden O, Sundqvist VA, Wahren B (1986) Clinical and subclinical reactivations of varicella-zoster virus in immunocompromised patients. J Infect Dis 153:840–847

Lohi H, Kujala M, Makela S, Lehtonen E, Kestila M, Saarialho-Kere U, Markovich D, Kere J (2002) Functional characterization of three novel tissue-specific anion exchangers SLC26A7, -A8, and -A9. J Biol Chem 277:14246–14254

Lungu O, Annunziato PW, Gershon A, Staugaitis SM, Josefson D, LaRussa P, Silverstein SJ (1995) Reactivated and latent varicella-zoster virus in human dorsal root ganglia. Proc Natl Acad Sci U S A 92:10980–10984

Maden M (2007) Retinoic acid in the development, regeneration and maintenance of the nervous system. Nat Rev Neurosci 8:755–765

Mahalingam R, Traina-Dorge V, Wellish M, Lorino R, Sanford R, Ribka EP, Alleman SJ, Brazeau E, Gilden DH (2007a) Simian varicella virus reactivation in cynomolgus monkeys. Virology

Mahalingam R, Traina-Dorge V, Wellish M, Lorino R, Sanford R, Ribka EP, Alleman SJ, Brazeau E, Gilden DH (2007b) Simian varicella virus reactivation in cynomolgus monkeys. Virology 368:50–59

Mahalingam R, Traina-Dorge V, Wellish M, Deharo E, Singletary ML, Ribka EP, Sanford R, Gilden D (2010) Latent simian varicella virus reactivates in monkeys treated with tacrolimus with or without exposure to irradiation. J Neurovirol 16:342–354

Malik AR, Urbanska M, Gozdz A, Swiech LJ, Nagalski A, Perycz M, Blazejczyk M, Jaworski J (2013) Cyr61, a matricellular protein, is needed for dendritic arborization of hippocampal neurons. J Biol Chem 288:8544–8559

Manteniotis S, Lehmann R, Flegel C, Vogel F, Hofreuter A, Schreiner BS, Altmuller J, Becker C, Schobel N, Hatt H, Gisselmann G (2013) Comprehensive RNA-Seq expression analysis of sensory ganglia with a focus on ion channels and GPCRs in trigeminal ganglia. PLoS One 8:e79523

Martin EA, Muralidhar S, Wang Z, Cervantes DC, Basu R, Taylor MR, Hunter J, Cutforth T, Wilke SA, Ghosh A, Williams ME (2015) The intellectual disability gene Kirrel3 regulates target-specific mossy fiber synapse development in the hippocampus. elife 4:e09395

Maze I, Wenderski W, Noh KM, Bagot RC, Tzavaras N, Purushothaman I, Elsasser SJ, Guo Y, Ionete C, Hurd YL, Tamminga CA, Halene T, Farrelly L, Soshnev AA, Wen D, Rafii S, Birtwistle MR, Akbarian S, Buchholz BA, Blitzer RD, Nestler EJ, Yuan ZF, Garcia BA, Shen L, Molina H, Allis CD (2015) Critical role of histone turnover in neuronal transcription and plasticity. Neuron 87:77–94

Mazzoni EO, Mahony S, Peljto M, Patel T, Thornton SR, McCuine S, Reeder C, Boyer LA, Young RA, Gifford DK, Wichterle H (2013) Saltatory remodeling of Hox chromatin in response to rostrocaudal patterning signals. Nat Neurosci 16:1191–1198

Messaoudi I, Barron A, Wellish M, Engelmann F, Legasse A, Planer S, Gilden D, Nikolich-Zugich J, Mahalingam R (2009) Simian varicella virus infection of rhesus macaques recapitulates essential features of varicella zoster virus infection in humans. PLoS Pathog 5: e1000657

Meyer C, Dewane J, Kerns A, Haberthur K, Barron A, Park B, Messaoudi I (2013) Age and immune status of rhesus macaques impact simian

varicella virus gene expression in sensory ganglia. J Virol 87:8294–8306

Miura T, Nishinaka T, Terada T (2008) Different functions between human monomeric carbonyl reductase 3 and carbonyl reductase 1. Mol Cell Biochem 315:113–121

Molyneux SD, Waterhouse PD, Shelton D, Shao YW, Watling CM, Tang QL, Harris IS, Dickson BC, Tharmapalan P, Sandve GK, Zhang X, Bailey SD, Berman H, Wunder JS, Izsvak Z, Lupien M, Mak TW, Khokha R (2014) Human somatic cell mutagenesis creates genetically tractable sarcomas. Nat Genet 46:964–972

Murali-Krishna K, Ahmed R (2000) Cutting edge: naive T cells masquerading as memory cells. J Immunol 165:1733–1737

Nagasawa K, Higashi T, Hosokawa N, Kaufman RJ, Nagata K (2007) Simultaneous induction of the four subunits of the TRAP complex by ER stress accelerates ER degradation. EMBO Rep 8:483–489

Neujahr DC, Chen C, Huang X, Markmann JF, Cobbold S, Waldmann H, Sayegh MH, Hancock WW, Turka LA (2006) Accelerated memory cell homeostasis during T cell depletion and approaches to overcome it. J Immunol 176:4632–4639

Novak MA, Hamel AF, Kelly BJ, Dettmer AM, Meyer JS (2013) Stress, the HPA axis, and nonhuman primate well-being: a review. Appl Anim Behav Sci 143:135–149

Oda K, Shiratsuchi T, Nishimori H, Inazawa J, Yoshikawa H, Taketani Y, Nakamura Y, Tokino T (1999) Identification of BAIAP2 (BAI-associated protein 2), a novel human homologue of hamster IRSp53, whose SH3 domain interacts with the cytoplasmic domain of BAI1. Cytogenet Cell Genet 84:75–82

O'Keeffe GW, Gutierrez H, Howard L, Laurie CW, Osorio C, Gavalda N, Wyatt SL, Davies AM (2016) Region-specific role of growth differentiation factor-5 in the establishment of sympathetic innervation. Neural Dev 11:4

Ono Y, Nakatani T, Minaki Y, Kumai M (2010) The basic helix-loop-helix transcription factor Nato3 controls neurogenic activity in mesencephalic floor plate cells. Development 137:1897–1906

Onozawa M, Hashino S, Takahata M, Fujisawa F, Kawamura T, Nakagawa M, Kahata K, Kondo T, Ota S, Tanaka J, Imamura M, Asaka M (2006) Relationship between preexisting anti-varicella-zoster virus (VZV) antibody and clinical VZV reactivation in hematopoietic stem cell transplantation recipients. J Clin Microbiol 44:4441–4443

Onunu AN, Uhunmwangho A (2004) Clinical spectrum of herpes zoster in HIV-infected versus non-HIV infected patients in Benin City, Nigeria. West Afr J Med 23:300–304

Ouwendijk WJ, Abendroth A, Traina-Dorge V, Getu S, Steain M, Wellish M, Andeweg AC, Osterhaus AD, Gilden D, Verjans GM, Mahalingam R (2013) T-cell infiltration correlates with CXCL10 expression in ganglia of cynomolgus macaques with reactivated simian varicella virus. J Virol 87:2979–2982

Oxman MN (2009) Herpes zoster pathogenesis and cell-mediated immunity and immunosenescence. J Am Osteopath Assoc 109:S13–S17

Park HB, Kim KC, Park JH, Kang TY, Lee HS, Kim TH, Jun JB, Bae SC, Yoo DH, Craft J, Jung S (2004) Association of reduced CD4 T cell responses specific to varicella zoster virus with high incidence of herpes zoster in patients with systemic lupus erythematosus. J Rheumatol 31:2151–2155

Pergam SA, Forsberg CW, Boeckh MJ, Maynard C, Limaye AP, Wald A, Smith NL, Young BA (2011) Herpes zoster incidence in a multicenter cohort of solid organ transplant recipients. Transpl Infect Dis 13:15–23

Rapino C, Bianchi G, Di Giulio C, Centurione L, Cacchio M, Antonucci A, Cataldi A (2005) HIF-1alpha cytoplasmic accumulation is associated with cell death in old rat cerebral cortex exposed to intermittent hypoxia. Aging Cell 4:177–185

Ray A, Treloar HB (2012) IgSF8: a developmentally and functionally regulated cell adhesion molecule in olfactory sensory neuron axons and synapses. Mol Cell Neurosci 50:238–249

Rege TA, Hagood JS (2006) Thy-1 as a regulator of cell-cell and cell-matrix interactions in axon regeneration, apoptosis, adhesion, migration, cancer, and fibrosis. FASEB J 20:1045–1054

Reichelt M, Zerboni L, Arvin AM (2008). Mechanisms of varicella-zoster virus neuropathogenesis in human dorsal root ganglia. J Virol 82: 3971–3983.

Reimers M, Schwarzenberger F, Preuschoft S (2007) Rehabilitation of research chimpanzees: stress and coping after long-term isolation. Horm Behav 51:428–435

Robinson MD, McCarthy DJ, Smyth GK (2010) edgeR: a Bioconductor package for differential expression analysis of digital gene expression data. Bioinformatics 26:139–140

Rusthoven JJ, Ahlgren P, Elhakim T, Pinfold P, Reid J, Stewart L, Feld R (1988) Varicella-zoster infection in adult cancer patients. A population study. Arch Intern Med 148:1561–1566

Schmader K (1998) Postherpetic neuralgia in immunocompetent elderly people. Vaccine 16:1768–1770

Schmader K, Studenski S, MacMillan J, Grufferman S, Cohen HJ (1990) Are stressful life events risk factors for herpes zoster? J Am Geriatr Soc 38:1188–1194

Sheu TT, Chiang BL, Yen JH, Lin WC (2014) Premature CD4+ T cell aging and its contribution to lymphopenia-induced proliferation of memory cells in autoimmune-prone non-obese diabetic mice. PLoS One 9:e89379

St Leger AJ, Hendricks RL (2011) CD8+ T cells patrol HSV-1-infected trigeminal ganglia and prevent viral reactivation. J Neurovirol 17:528–534

Strezoska Z, Pestov DG, Lau LF (2000) Bop1 is a mouse WD40 repeat nucleolar protein involved in 28S and 5. 8S RRNA processing and 60S ribosome biogenesis. Mol Cell Biol 20:5516–5528

Terada K, Kawano S, Yoshihiro K, Morita T (1994) Varicella-zoster virus (VZV) reactivation is related to the low response of VZV-specific immunity after chickenpox in infancy. J Infect Dis 169:650–652

Toth C, Shim SY, Wang J, Jiang Y, Neumayer G, Belzil C, Liu WQ, Martinez J, Zochodne D, Nguyen MD (2008) Ndel1 promotes axon regeneration via intermediate filaments. PLoS One 3:e2014

Traina-Dorge V, Doyle-Meyers LA, Sanford R, Manfredo J, Blackmon A, Wellish M, James S, Alvarez X, Midkiff C, Palmer BE, Deharo E, Gilden D, Mahalingam R (2015) Simian varicella virus is present in macrophages, dendritic cells, and T cells in lymph nodes of rhesus macaques after experimental reactivation. J Virol 89:9817–9824

Uchakin PN, Parish DC, Dane FC, Uchakina ON, Scheetz AP, Agarwal NK, Smith BE (2011) Fatigue in medical residents leads to reactivation of herpes virus latency. Interdiscip Perspect Infect Dis 2011:571340

Vallortigara J, Chassande O, Higueret P, Enderlin V (2009) Thyroid hormone receptor alpha plays an essential role in the normalisation of adult-onset hypothyroidism-related hypoexpression of synaptic plasticity target genes in striatum. J Neuroendocrinol 21:49–56

Vermont CL, Jol-van der Zijde EC, Hissink Muller P, Ball LM, Bredius RG, Vossen AC, Lankester AC (2014) Varicella zoster reactivation after hematopoietic stem cell transplant in children is strongly correlated with leukemia treatment and suppression of host T-lymphocyte immunity. Transpl Infect Dis 16:188–194

Wang CC, Kadota M, Nishigaki R, Kazuki Y, Shirayoshi Y, Rogers MS, Gojobori T, Ikeo K, Oshimura M (2004) Molecular hierarchy in neurons differentiated from mouse ES cells containing a single human chromosome 21. Biochem Biophys Res Commun 314:335–350

Weinberg A, Zhang JH, Oxman MN, Johnson GR, Hayward AR, Caulfield MJ, Irwin MR, Clair J, Smith JG, Stanley H, Marchese RD, Harbecke R, Williams HM, Chan IS, Arbeit RD, Gershon AA, Schodel F, Morrison VA, Kauffman CA, Straus SE, Schmader KE, Davis LE, Levin MJ (2009) Varicella-zoster virus-specific immune responses to herpes zoster in elderly participants in a trial of a clinically effective zoster vaccine. J Infect Dis 200:1068–1077

Westerlund N, Zdrojewska J, Padzik A, Komulainen E, Bjorkblom B, Rannikko E, Tararuk T, Garcia-Frigola C, Sandholm J, Nguyen L, Kallunki T, Courtney MJ, Coffey ET (2011) Phosphorylation of SCG10/stathmin-2 determines multipolar stage exit and neuronal migration rate. Nat Neurosci 14:305–313

Wieczorek E, Brand M, Jacq X, Tora L (1998) Function of TAF(II)-containing complex without TBP in transcription by RNA polymerase II. Nature 393:187–191

Wilson JF, Marsa GW, Johnson RE (1972) Herpes zoster in Hodgkin's disease. Clinical, histologic, and immunologic correlations. Cancer 29:461–465

Yamaguchi M, Yu S, Qiao R, Weissmann F, Miller DJ, VanderLinden R, Brown NG, Frye JJ, Peters JM, Schulman BA (2015) Structure of an APC3-APC16 complex: insights into assembly of the anaphase-promoting complex/cyclosome. J Mol Biol 427:1748–1764

Yawn BP, Wollan PC, Kurland MJ, St Sauver JL, Saddier P (2011) Herpes zoster recurrences more frequent than previously reported. Mayo Clin Proc 86:88–93

Yik JH, Chen R, Pezda AC, Zhou Q (2005) Compensatory contributions of HEXIM1 and HEXIM2 in maintaining the balance of active and inactive positive transcription elongation factor b complexes for control of transcription. J Biol Chem 280:16368–16376

Yorimitsu T, Sato K, Takeuchi M (2014) Molecular mechanisms of Sar/Arf GTPases in vesicular trafficking in yeast and plants. Front Plant Sci 5:411

Zhang D, Zhao T, Ang HS, Chong P, Saiki R, Igarashi K, Yang H, Vardy LA (2012) AMD1 is essential for ESC self-renewal and is translationally down-regulated on differentiation to neural precursor cells. Genes Dev 26:461–473

Zhang T, Wang Z, Wang L, Luo N, Jiang L, Liu Z, Wu CF, Dong K (2013) Role of the DSC1 channel in regulating neuronal excitability in *Drosophila melanogaster*: extending nervous system stability under stress. PLoS Genet 9:e1003327